This article has been accepted for publication in a future issue of this journal, but has not been fully edited. Content may change prior to final publication. Citation information: DOI 10.1109/ACCESS.2021.3117839, IEEE Access

IEEE Access
Multidisciplinary | Rapid Review | Open Access Journal

Thermal analysis of conductive-convective-radiative heat exchangers with temperature dependent thermal conductivity

NAVEED AHMAD KHAN[1], MUHAMMAD SULAIMAN[*1], POOM KUMAM[*2,3,4], (Member, IEEE), MAHARANI A. BAKAR[5]

[1]Department of Mathematics, Abdul Wali Khan University, Mardan 23200, KP, Pakistan (e-mail: ashfaq.maths@yahoo.com)
[2]KMUTT Fixed Point Research Laboratory, KMUTT-Fixed Point Theory and Applications Research Group, SCL 802 Fixed Point Laboratory, Department of Mathematics, Faculty of Science, King Mongkut's University of Technology Thonburi (KMUTT), 126 Pracha Uthit Rd., Bang Mod, Thung Khru, Bangkok 10140, Thailand
[3]Center of Excellence in Theoretical and Computational Science (TaCS-CoE), SCL 802 Fixed Point Laboratory, Science Laboratory Building, King Mongkut's University of Technology Thonburi (KMUTT), 126 Pracha-Uthit Road, Bang Mod, Thrung Khru, Bangkok 10140, Thailand
[4]Department of Medical Research, China Medical University Hospital, China Medical University, Taichung 40402, Taiwan.
[5]Applied Mathematics and Scientific Computing Research Interest Group, Faculty of Ocean Engineering Technology and Informatics, Universiti Malaysia Terengganu, Kuala Nerus, Terengganu 21300, Malaysia.

Corresponding author: (M. Sulaiman msulaiman@awkum.edu.pk, Poom Kumam poom.kum@kmutt.ac.th)

The authors acknowledge the financial support provided by the Center of Excellence in Theoretical and Computational Science (TaCS-CoE), KMUTT.

ABSTRACT In this paper, one dimensional mathematical model of convective-conductive-radiative fins is presented with thermal conductivity depending on temperature. The temperature field with insulated tip is determined for a fin in convective, conductive and radiative environments. Moreover, an intelligent soft computing paradigm named as the LeNN-WOA-NM algorithm is designed to analyze the mathematical model for the temperature field of convective-conductive-radiative fins. The proposed algorithm uses function approximating ability of Legendre polynomials based on artificial neural networks (ANN's), global search optimization ability of Whale optimization algorithm (WOA), and local search convergence of Nelder-Mead algorithm. The proposed algorithm is applied to illustrate the effect of variations in coefficients of convection, radiation heat losses, and dimensionless parameter of thermal conductivity on temperature distribution of conductive-convective and radiative fins in convective and radiative environments. The experimental data establishes the effectiveness of the design scheme when compared with techniques in the latest literature. It can be observed that accuracy of approximate temperature increases with lower values of N_c and N_r while decreases with increase in λ. The quality of solutions obtained by LeNN-WOA-NM algorithm are validated through performance indicators including absolute errors, MAD, TIC, and ENSE.

INDEX TERMS Conductive-convective-radiative fin, Temperature-dependent thermal conductivity, Temperature distribution, Weighted Legendre neural networks, Hybrid soft computing, Whale optimization algorithm, Nelder Mead algorithm.

I. INTRODUCTION

HEAT exchangers or fins are also known as extended surfaces which are commonly used as an element of heat dissipation, that improves the performance and efficiency of equipments [1]. Fins have various applications in air conditioning, energy systems equipment, chemical processes, heat exchanger, cooling systems for computer equipment and refrigeration. Extended surfaces or fins are designed in different shapes for a class of longitudinal fins with a cross section much less than one dimensional (1D) extended surfaces or length directional. In particular, temperature-dependent behavior is revealed by thermal conductivity when dramatic changes in temperature of the fins occurred. This results in a nonlinear fin problem. Another source of nonlinearity arises from radiation. For example, measurable results from an experiment reveal that heat loss due to radiation is around

15–20 percent of the total heat loss along a fin cooled by natural convection and radiation [2]. As a result, radiation heat transfer has a significant impact on heat exchanger performance, particularly at high temperatures [3]. Thus, similar to conduction and convection, radiation has a substantial influence on temperature distribution and is important for increasing the thermal efficiency of fins, especially for devices with a low convection heat transfer coefficient. Heat transfer in fins is related to one dimensional nonlinear problem, where heat transfer coefficient and thermal conductivity are temperature dependent. Effect of variations in thermal conductivity and heat transfer of several nonlinear models has been extensively studied in [4]–[10]. Various techniques have been designed to study the approximate temperature distribution of extended surfaces in convective-conductive nonlinear fin problems. Chiu [11] and Arsalan [12] proposed Adomain decomposition method to model analytical solution in the form of power series. In addition, other numerical methods that are used to find temperature distribution of fins are homotopy perturbation method [13], [14], homotopy analysis method [15], variational iteration method [16], [17], differential transformation method [18], Galerkin's method [19] and the series method [20]. R.J. Moitsheki [21] applied classical Lie symmetry techniques to find exact solutions of the fin problem with a power-law temperature-dependent thermal conductivity. Abbas [22] in 2017 calculate closed-form solutions for heat transfer in a straight fin. In recent times, Sheng-Wei Sun [23] studied the exact solution of the nonlinear fin problem with exponentially temperature-dependent thermal conductivity and heat transfer coefficient. [24]–[30] recently focused on the study of optimization of various nonlinear models representing physical phenomenon. Radiation, in addition to convection, is another source of heat loss. When heat loss through natural convection is comparable to heat loss from an extended (fin) surface, radiation heat loss cannot be neglected. Thus, for the devices having a low convection heat transfer coefficient, convection and radiation heat transfer coefficients play a vital role. Convection and radiation heat transfer must be used to evaluate high performances of convective, conductive, and radiative extend surfaces (fins). Meanwhile, a strong nonlinear impact on temperature is exhibited by radiation heat loss transfer. Most of above listed methods have been designed to study the thermal distribution and performance of conductive, convective and radiative extend surfaces. DTM method is developed by [31] to study convective and radiative fins with thermal conductivity depending on temperature. [32] find the series solution for convective radiative conduction equation of nonlinear fin with temperature-dependent thermal conductivity. [33] studies a radial fin of uniform thickness with convective heating at the base and convective–radiative cooling at the tip. Generalized variational iteration method is used by Miansari [34] to deal with nonlinear fin problem with radiation heat loss. Atouei uses collocation method [35], Runge-Kutta method [36] and least square method [37] to analyze temperature distribution and performance of radiative-convective semi-spherical extended surfaces. Optimal linearization method (OLM) [38] was developed to find approximate solutions for temperature field in convective and radiative heat transfers. An integral equation method is introduced by Y. Huang [39] to find an analytical and approximate distribution of temperature and fin performance for convective, conductive, and radiative fin. Multiple shape fins along with longitudinal fins has been widely studied such as T-shaped fins [40], [41], 2D orthotropic convection pin fin [42], [43] and stepped fins [44], [45]. By considering, Cattaneo-Christov heat flux model T. Hayat [28], [46] studied the impact of variable thermal conductivity over a variable thick surfaces. The classical lie point symmetry method is applied by Mhlongo [47] to investigate the behavior of temperature when subjected to heat flow jump and base temperature jump. [48], [49] analyzed the mathematical model of non-Fourier heat conduction on wet extended surfaces.

In recent times, the heat transfer performance of fin gained the attention of researchers due to dramatic changes in the behavior of fin with temperature variations. Thus, it becomes necessary to design a method that can easily calculate the distribution of temperature in a fin. Unlike approaches available in the literature, this paper focuses on strengthening the concept of artificial neural networks (ANN's). ANN based meta heuristic algorithms are used to solve variety of nonlinear problems arising in fluid dynamics [50]–[54], civil engineering [55], [56], wire coating dynamics [57], thermal engineering [58], [59], biomathematics [60]–[62], financial marketing [63]–[65], fuzzy systems [66]–[68] and petroleum engineering [69]. These potential application of stochastic techniques encourage the authors to strengthen computational ability of ANN's based on Legendre neural networks to study the temperature distribution of fins. The innovative contribution of the given study are summarized as follows:

- A mathematical model for temperature distribution of fin with thermal conductivity in the conductive, convective and radiative environment is presented.
- A novel computing paradigm is design by using function approximating ability of orthogonal Legendre polynomials with hybridization of the Whale optimization algorithm (WOA) and the Nelder-Mead algorithm (NM). Proposed methodology is named as LeNN-WOA-NM.
- Further, the design scheme is utilized to study the influence of variations in coefficient of radiation and convection.
- The results obtained by design soft computing paradigm are compared with integral method and exact solution which shows the accuracy of design algorithm with minimum absolute errors in the solutions.
- Verification and validation of the performance analysis based on statistics in terms of standard deviations, mean absolute deviations, absolute errors, Theil's inequality coefficient, variance and error in Nash Sutcliffe efficiency for design scheme have been evaluated by executing LeNN-WOA-NM algorithm for 100 independent runs.

This article has been accepted for publication in a future issue of this journal, but has not been fully edited. Content may change prior to final publication. Citation information: DOI 10.1109/ACCESS.2021.3117839, IEEE Access

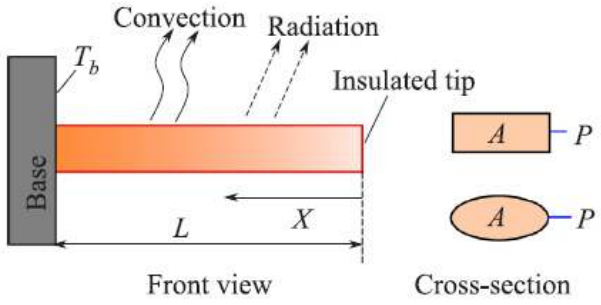

FIGURE 1. Schematic of a conductive, convective and radiative fin.

II. PROBLEM FORMULATION

Consider a conductive-convective-radiative fin of length L and cross-sectional A with a temperature-dependent thermal conductivity shown in Figure 1. It is assumed that the fin is made of isotropic solid material relatively long compared to its cross-section. Moreover, the temperature at the base of the fin in a convection environment is considered uniform. By convection-radiation, heat is dissipated on the surface of a fin, and heat transfer through the tip of the fin is neglected. Stefan-Boltzmann's law is obeyed by radiation when heat is dissipated from the surface of fins. During the process, the fin is at rest while heat flows in a steady state. Over the entire surface of the fin, convection heat transfer coefficient N_c is considered to be uniform while thermal conductivity $k(T)$ depends on temperature, which is defined as [70]

$$k(T) = k\left[1 + \lambda'\left(T - T_a\right)\right], \tag{1}$$

where ambient temperature is presented by T_a. When inner temperature T of fins is equal to ambient temperature $(T = T_a)$ then k denotes thermal conductivity. Temperature change is denoted by λ' . At any cross section during flow of heat, T is invariant and varies only with longitudinal directions. Therefore, the phenomena presented in Figure 1 satisfies one dimensional non-linear differential equation for heat transfer which is given by Eq (2) [22].

$$\frac{d}{dX}\left(k(T)A\frac{dT}{dX}\right) - Ph\left(T - T_a\right) - \varepsilon\sigma P\left(T^4 - T_s^4\right) = 0, \tag{2}$$

where $0 < X < L$, ϵ is surface emissivity, h is convection heat transfer coefficient, Stefan-Boltzmann constant is denoted by ρ and sink temperature for radiation is presented by T_s. Now, introducing non-dimensional variables as follows

$$\theta = \frac{T - T_a}{T_b - T_a}, \quad x = \frac{X}{L}, \quad l = \frac{LP}{A}, \tag{3}$$

$$N_c = l^2\frac{hA}{kP}, \quad N_r = l^2\frac{\varepsilon\sigma AT_b^3}{kP}, \quad \lambda = \lambda'\left(T_b - T_a\right), \tag{4}$$

temperature at base of fin is denoted by T_b and λ is dimensionless parameter so, Eq (2) can be written as

$$\frac{d}{dx}\left((1 + \lambda\theta)\frac{d\theta}{dx}\right) - N_c\theta - N_r\theta^4 = 0, \quad 0 < x < 1, \tag{5}$$

further, Eq (5) can be simplified to [71]

$$\frac{d^2\theta}{dx^2} + \lambda\theta\frac{d^2\theta}{dx^2} + \lambda\left(\frac{d\theta}{dx}\right)^2 - N_c\theta - N_r\theta^4 = 0, \quad 0 < x < 1, \tag{6}$$

at fin tip $(x = 0)$, loss of heat is negligible therefore, it is assumed to be insulated. The boundary conditions for conductive,convective and radiative fin with thermal conductivity can be defined as [11], [72]

$$\frac{d\theta}{dx}(0) = 0, \quad \theta(1) = 1. \tag{7}$$

Despite exact solutions found by [21], [22], [39] for Eq (6) with boundary conditions Eq (7), a novel soft computing technique known as LeNN-WOA-NM algorithm is designed to find analytical solution for conductive,convective and radiative fin with thermal conductivity.

III. APPROXIMATE SOLUTION AND WEIGHTED LEGENDRE NEURAL NETWORK (LENN) MODAL

The Legendre polynomials are denoted by $L_n(x)$, where n denotes order of Legendre polynomials. The set $L_1, L_2, L_3, \ldots, L_n$ constitutes the set of orthogonal polynomials on $[-1, 1]$. First eleven Legendre polynomials are given in Table 1 . Higher order Legendre polynomials are generated

TABLE 1. Legendre polynomials.

n	$L_n(x)$
0	1
1	x
2	$\frac{1}{2}\left(3x^2 - 1\right)$
3	$\frac{1}{2}\left(5x^3 - 3x\right)$
4	$\frac{1}{8}\left(35x^4 - 30x^2 + 3\right)$
5	$\frac{1}{8}\left(63x^5 - 70x^3 + 15x\right)$
6	$\frac{1}{16}\left(231x^6 - 315x^4 + 105x^2 - 5\right)$
7	$\frac{1}{16}\left(429x^7 - 693x^5 + 315x^3 - 35x\right)$
8	$\frac{1}{128}\left(6435x^8 - 12012x^6 + 6930x^4 - 1260x^2 + 35\right)$
9	$\frac{1}{128}\left(12155x^9 - 25740x^7 + 18018x^5 - 4620x^3 + 315x\right)$
10	$\frac{1}{256}\left(46189x^{10} - 109395x^8 + 90090x^6 - 30030x^4 + 3465x^2 - 63\right)$

by using a recursive relation given by Eq (8) [72].

$$L_{n+1}(x) = \frac{1}{n+1}\left[(2n+1)xL_n(x) - nL_{n-1}(x)\right], \tag{8}$$

We consider trial solution for Eq (6) presenting non-linear fin problem with temperature dependent thermal conductivity as

$$\theta_{approx}(x) = \sum_{n=0}^{N}\delta_n L_n\left(\psi_n x + \xi_n\right), \tag{9}$$

where δ_n, ψ_n and ξ_n are unknown neurons that would be determined in course of solution. Figure 2 shows structure of Legendre neural networks. As Eq (9) is continuous and differentiable therefore θ' and θ'' can be calculated as following

$$\theta'_{approx}(x) = \sum_{n=1}^{N}\delta_n L'_n\left(\psi_n x + \xi_n\right), \tag{10}$$

This article has been accepted for publication in a future issue of this journal, but has not been fully edited. Content may change prior to final publication. Citation information: DOI 10.1109/ACCESS.2021.3117839, IEEE Access

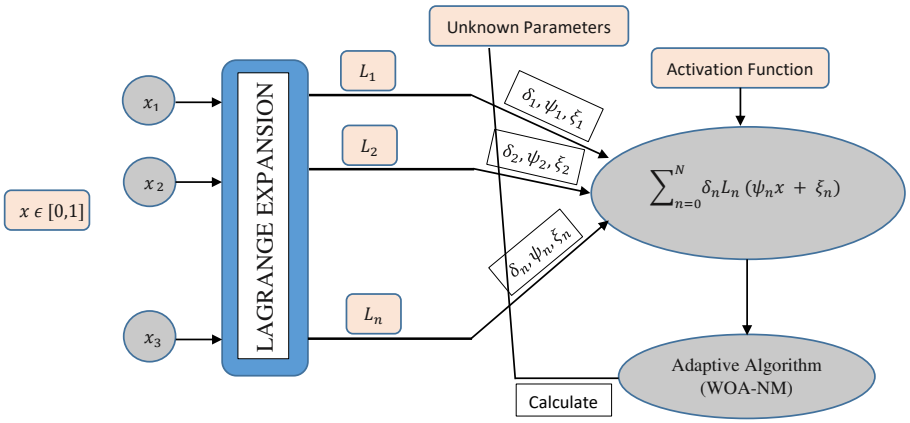

FIGURE 2. Structure of Legendre Neural Network modal.

$$\theta''_{approx}(x) = \sum_{n=4}^{N} \delta_n L''_n (\psi_n x + \xi_n). \tag{11}$$

Plugging, θ, θ' and θ'' in Eq (6) will model governing differential equation of conductive, convective and radiative fins. Mathematical model in terms of input, hidden and output layers is shown in Figure 4.

A. THE WHALE OPTIMIZATION ALGORITHM

Whale optimization algorithm (WOA) is a nature-inspired stochastic optimization technique developed by Mirjalili and Lewis [73] which mimics the foraging of humpback whales. It is a global search optimizer that utilizes population search space to determine the global optimum solution for optimization problems. Likewise, other population-based metaheuristic algorithms, WOA, start optimizing the given problem by generating random candidate solutions. It then improves the set with each iteration until a satisfaction criterion for an ending is achieved. WOA is inspired by the bubble net hunting strategy of humpback whales as shown in Figure 3.

From Figure 3(b) it can be observed that hump back whales encircles the prey by moving in spiral path and creating bubbles along the way. The mathematical model for bubble net mechanism is given by

$$\vec{X}(t+1) = \begin{cases} \vec{X}^*(t) - \vec{A} \cdot D, & \text{if } p < 0.5 \\ D' \cdot e^{bl} \cdot \cos(2\pi l) + \overrightarrow{X^*}(t) & \text{if } p \geq 0.5, \end{cases} \tag{12}$$

where "p" is a random value in [0,1], b is shape of logarithmic spiral and l is a random number in [-1,1]. X^* represents best solution obtained so far while D and D' are defined by following equations

$$D = |\vec{C} \cdot \overrightarrow{X_{\text{rand}}} - \vec{X}|, \tag{13}$$

$$D' = |\overrightarrow{X^*}(t) - \vec{X}(t)|, \tag{14}$$

$\vec{A}$ and $\vec{C}$ are coefficient vectors and given as follows:

$$\vec{A} = 2\vec{a} \cdot \vec{r} - \vec{a}, \tag{15}$$

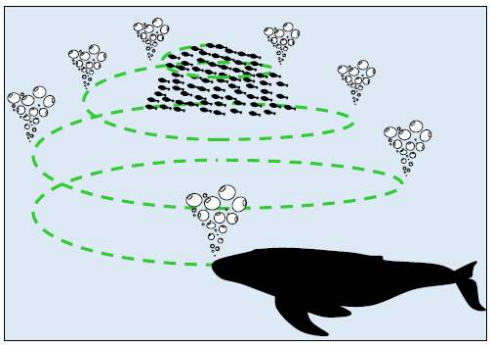

(a) Bubble-net behavior of humpback whales in nature

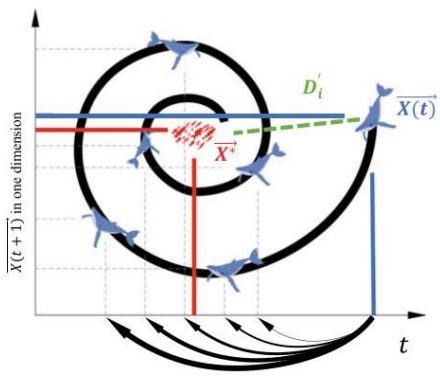

(b) The spiral movement of humpback whales

FIGURE 3. Bubble-net search mechanism implemented in WOA (a) shrinking encircling mechanism and (b) spiral updating position.

$$\vec{C} = 2 \cdot \vec{r}. \tag{16}$$

r is a random vector between [0,1] and a decreases linearly from 2 to 0 with the course of iterations.

The first component of Eq (12) illustrates the encircling mechanism, whereas the second mimics the bubble-net strategy. The variable p switches between these two components with an equal probability. Output X^* depends on the value of p. WOA starts the process with a set of random solutions. At each iteration, update the position of search agents with

This article has been accepted for publication in a future issue of this journal, but has not been fully edited. Content may change prior to final publication. Citation information: DOI 10.1109/ACCESS.2021.3117839, IEEE Access

respect to either a randomly chosen search agent or the best solution obtained so far. Working procedure of the WOA is shown through flow chart in Figure 5. Initial parameter setting for WOA is given in Table 2.

B. NELDER-MEAD ALGORITHM

Nelder-Mead (NM) algorithm is a direct search method known as the downhill simplex method developed by Nelder and Mead in 1965 to solve different problems without any information about the gradient [74]. NM is a single path following a local search optimizer that can find good results if initialized with a better initial solution. A simplex consisting of $n+1$ vertices is set up to minimize a function f with n dimensions [75]. NM algorithm generates a sequence of simplices by following four basic steps, named reflection, expansion, contraction, and shrink. Initially, the points $\left(x^1, x^2, \ldots, x^{n+1}\right)$ are generated and corresponding values of objective function are evaluated.

Sorting: Objective values for corresponding vertices of simplex are sorted to obtain centroid (x^0), worst (x^h), next to worst (x^{nw}) and best (x^b) values in all points.

Reflection: In this step, reflection point x^r is determined by Eq (17).

$$x^r = x^0 + \alpha\left(x^0 - x^h\right), \tag{17}$$

where α is reflection coefficient. If $f\left(x^1\right) \leq f\left(x^r\right) < f\left(x_{n+1}\right)$ then iteration is terminated and "x^r" is accepted.

Expansion: The expansion point x^e is computed by using the equation given below

$$x^e = x^0 + \gamma\left(x^r - x^0\right), \tag{18}$$

If $f\left(x^e\right) \leq f\left(x^r\right)$ then x^e would be accepted and iteration will be stopped.

Contraction: If objective value at x^r is strictly greater then objective value at x^{nw} then this steps contraction is applied.

a) If $f\left(x^r\right) < f(x^h)$ then the outside contraction is applied by using Eq. (19).

$$x^{oc} = x^0 + \beta\left(x^r - x^0\right), \tag{19}$$

β is an expansion coefficient b) If $f\left(x^r\right) > f(x^h)$ then the inside contraction is applied by using Eq. (20).

$$x^{ic} = x^0 + \beta\left(x^h - x^0\right), \tag{20}$$

Shrinkage: It is a final step and the result is calculated by Eq. (21).

$$x^i = x^i + \gamma\left(x^b - x^i\right). \tag{21}$$

where δ is shrink coefficient. The resulting simplex generated by NM algorithm for succeeding iterations can be written as $X = x^i, i = 1, 2, 3, \ldots, n+1$. Parameter setting for Nelder-Mead algorithm are given in Table 2.

IV. LENN-WOA-NM ALGORITHM

The steps for the proposed hybridized algorithm are summarized as:

Step 1: Initialization: Randomly generates an initial population using Eq (9), with number of parameters equal to number of neurons in LeNN's structure. Parameters setting to initialize WOA is demonstrated in Table 2.

Step 2: Fitness evaluation: Calculate the fitness value for each individual of candidate space by using Eq (22).

Step 3: Termination criteria: Terminate the process of fitness evaluation, if any of the following termination criteria is achieved.

- When maximum number of predefined iterations in achieved.
- When fitness value $\epsilon \leq 10^{-25}$.

Step 4: Ranking: Rank the individuals of the population on the basis of values of the fitness function ϵ.

Step 5: Storage: Store the values of weights and fitness function.

Step 6: Initialization of NM : Nelder-Mead algorithm is used for further speedy fine tuning of the results, starting with global best values of δ_n, ψ_n and ξ_n obtained by WOA. Parameters setting for NM algorithm is shown in Table 2.

Step 7: Refinement: NM algorithm uses MATLAB built in function "FMINSEARCH" to update the weights and evaluate the fitness function using Eq (22). The execution of the process stops when predefined stopping criteria is attained.

Step 8: Storage: Store the refined best values of ζ_n, ψ_n and θ_n along with fitness. The procedure in executed for 100 independent runs to obtain large set of statistical data.

LeNN-WOA-NM algorithm has a simple structure and easy to implement. WOA updates the position of individual using global search ability and bubble net strategy of humpback whales while NM algorithm further complements its local convergence. Since, Legendre polynomials are orthogonal on $[-1, 1]$ so the experimental analysis shows that proposed algorithm converges to best solutions for number of real-world problems by training the weights from the interval $[-1, 1]$. It has been notices that convergence of design scheme is slightly effected by increasing the domain.

V. CONSTRUCTION OF FITNESS FUNCTION

Fitness function ϵ is formulated on the basis of an unsupervised error, which is defined as the sum of mean square errors of Eq (6) and Eq (7) as

$$\text{Minimize } \epsilon = \widehat{\epsilon}_1 + \widehat{\epsilon}_2, \tag{22}$$

$$\begin{aligned}\text{Minimize } \epsilon =& \frac{1}{N}\sum_{m=1}^{N}\left(\begin{array}{c}\frac{d^2\theta_m}{dx^2} + \lambda\theta_m\frac{d^2\theta_m}{dx^2} + \lambda\left(\frac{d\theta_m}{dx}\right)^2 \\ -N_c\theta_m - N_r\theta_m^4\end{array}\right)^2 \\ &+ \frac{1}{2}\left(\left(\frac{d\theta}{dx}(0)\right)^2 + (\theta(1)-1)^2\right),\end{aligned} \tag{23}$$

where $N = \frac{1}{h}$ and h is a step size.

This article has been accepted for publication in a future issue of this journal, but has not been fully edited. Content may change prior to final publication. Citation information: DOI 10.1109/ACCESS.2021.3117839, IEEE Access

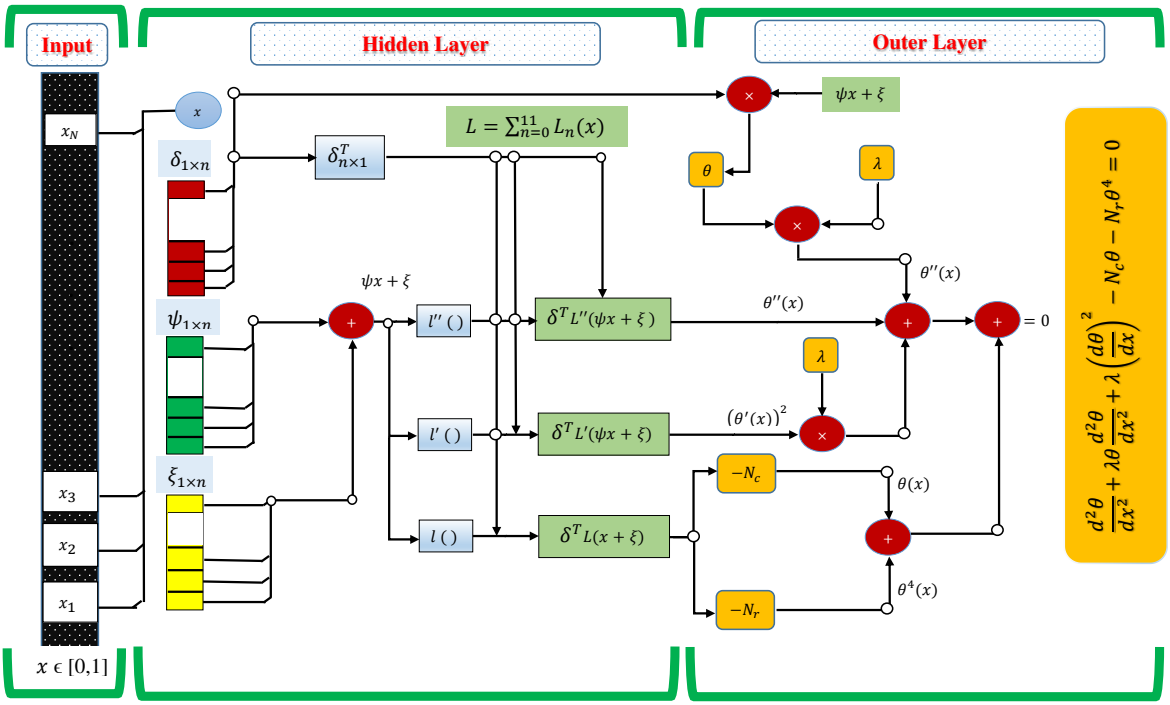

FIGURE 4. Structure of Legendre polynomials based neural networks for conductive-convective and radiative fins.

TABLE 2. Description of parameter settings for design algorithm.

Algorithm	Parameters	Settings	Parameters	Settings
LeNN-WOA	Technique	Metaheuristic	Candidate selection	Random search
	Max. Iterations	5,000	Function tolerance	10^{-18}
	Bounds (Lb, Ub)	[-1,1]	Fitness Limit	10^{-20}
	Search agents	70	Other settings	Default
NM	Initialization	Global best solution of WOA	X-Tolerance 'TolX'	1.00E-20
	Function evaluations	150,000	Max. iter	2,000
	Fitness Limit	10^{-20}	Other settings	Default

VI. PERFORMANCE MEASURES

To examine the accuracy and convergence of design scheme (LeNN-WOA-NM), in obtaining solutions for different problems of conductive-convective and radiative fins with thermal conductivity, performance measures are defined in term of fitness evaluation, mean absolute deviation (MAD), Theil's inequality coefficient (TIC) and error in Nash Sutcliffe efficiency (ENSE). Mathematical formulation for these indices are given below [69].

$$\text{MAD} = \frac{1}{n}\sum_{m=1}^{n} \left|\theta(x) - \theta_{approx}(x)\right|, \tag{24}$$

$$\text{TIC} = \frac{\sqrt{\frac{1}{n}\sum_{n=1}^{n}\left(\theta(x) - \theta_{approx}(x)\right)^2}}{\left(\sqrt{\frac{1}{n}\sum_{n=1}^{n}(\theta(x))^2} + \sqrt{\frac{1}{n}\sum_{n=1}^{n}(\theta_{approx}(x))^2}\right)}, \tag{25}$$

$$\text{NSE} = \left\{1 - \frac{\sum_{n=1}^{n}\left(\theta(x) - \theta_{approx}(x)\right)^2}{\sum_{n=1}^{n}\left(\left(\theta(x) - \widehat{\theta}(x)\right)^2\right.}, \widehat{\theta}(x) = \frac{1}{n}\sum_{m=1}^{n}\theta(x), \right. \tag{26}$$

$$ENSE = 1 - NSE. \tag{27}$$

where, n denote a grid points.

VII. NUMERICAL EXPERIMENTATION

In this section, we have defined different problems to study the influence of variations in coefficients of convective heat loss N_c, coefficient of radiative heat lost N_r and dimensionless parameter of thermal conductivity λ on temperature distribution of conductive-convective-radiative fins with thermal conductivity. Problems along with different cases studied in

This article has been accepted for publication in a future issue of this journal, but has not been fully edited. Content may change prior to final publication. Citation information: DOI 10.1109/ACCESS.2021.3117839, IEEE Access

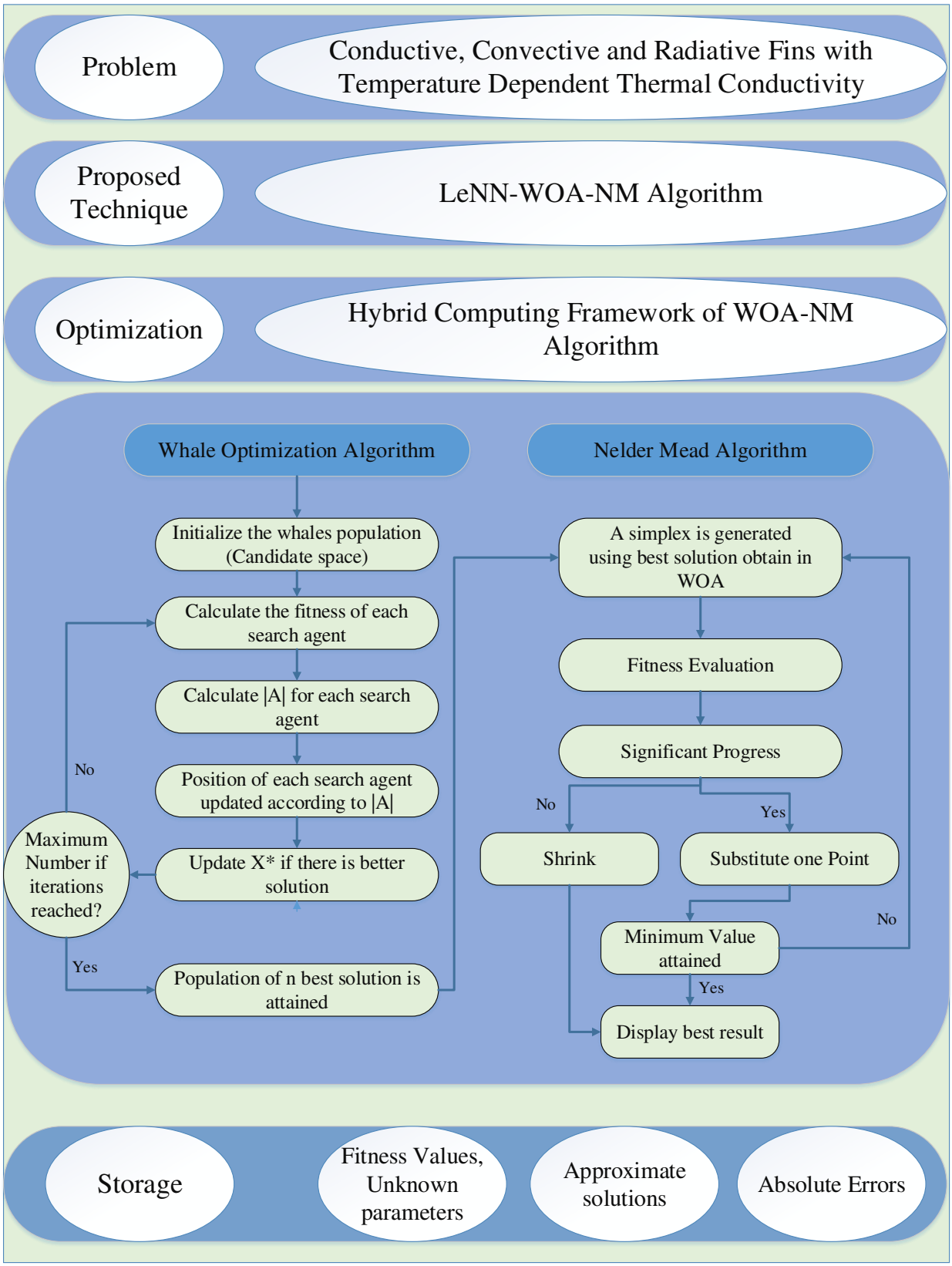

FIGURE 5. Graphical overview of WOA-NM Algorithm

This article has been accepted for publication in a future issue of this journal, but has not been fully edited. Content may change prior to final publication. Citation information: DOI 10.1109/ACCESS.2021.3117839, IEEE Access

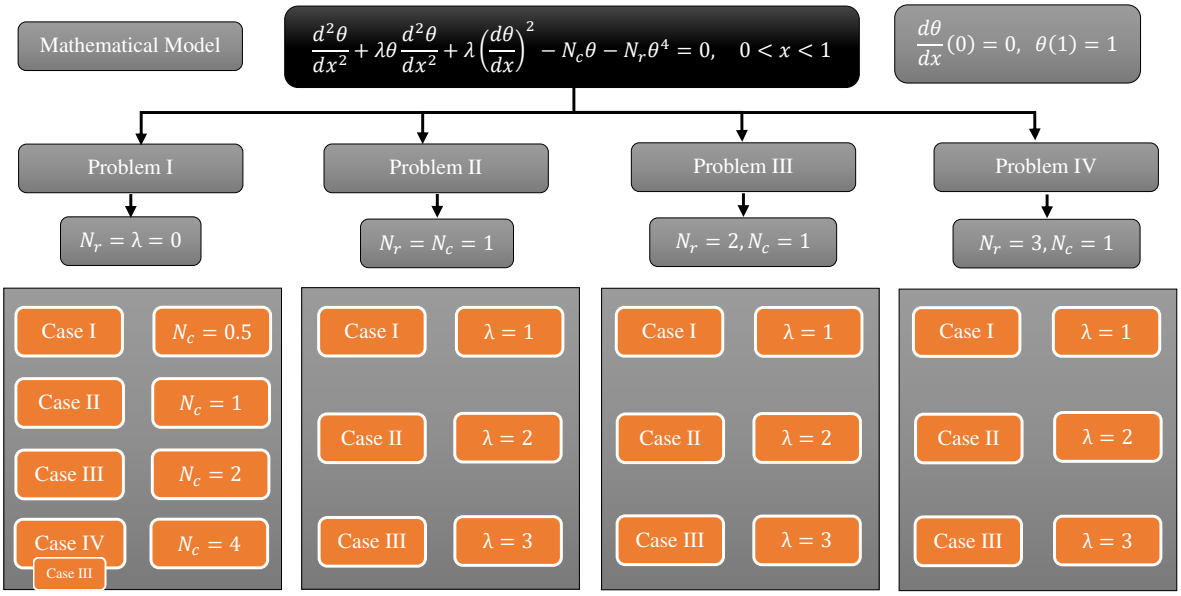

FIGURE 6. Graphical overview of problems along with different cases studied in this paper.

this paper are presented in the flow chart through Figure 6.

Problem I : Effect of Variations in N_c on temperature distribution with no resemblance of radiation heat loss and λ.

In this problem, the proposed technique is applied to study the influence of N_c on temperature distribution of fins with neglected radiation heat loss $N_r = 0$ and dimensionless parameter of thermal conductivity $\lambda = 0$. The fitness function for this problem is formulated as

$$\epsilon = \frac{1}{N}\sum_{m=1}^{N}\left(\frac{d^2\theta_m}{dx^2} - N_c\theta_m\right)^2 + \frac{1}{2}\left(\left(\theta'(0)\right)^2 + (\theta(1)-1)^2\right), \tag{28}$$

where $0 \leq x \leq 1$. Following four cases are considered.
Case I: Eq (28) with $N_c = 0.5$.
Case II: Eq (28) with $N_c = 1.0$.
Case III: Eq (28) with $N_c = 2.0$.
Case IV: Eq (28) with $N_c = 4.0$.

Problem II : Effect of Variations in dimensionless parameter of thermal conductivity λ on temperature distribution with $N_c = N_r = 1$.

In this problem, influence of variations in λ on temperature distribution of conductive, convective and radiative fins is considered with $N_c = N_r = 1$. Fitness function for this problem is formulated as

$$\text{Minimize } \epsilon = \frac{1}{N}\sum_{m=1}^{N}\left(\frac{d^2\theta_m}{dx^2} + \lambda\theta_m\frac{d^2\theta_m}{dx^2} + \lambda\left(\frac{d\theta_m}{dx}\right)^2 - \theta_m - \theta_m^4\right)^2 + \frac{1}{2}\left(\left(\frac{d\theta}{dx}(0)\right)^2 + (\theta(1)-1)^2\right), \tag{29}$$

where $0 \leq x \leq 1$, different cases for Eq (29) depending on dimensionless parameter of thermal conductivity are considered as follows.
Case I: Eq (29) with $\lambda = 1.0$.
Case II: Eq (29) with $\lambda = 2.0$.
Case III: Eq (29) with $\lambda = 3.0$.

Problem III : Effect of Variations in dimensionless parameter of thermal conductivity λ on temperature distribution with $N_c = 1$ and $N_r = 2$.
In this problem, influence of variations in dimensionless parameter of thermal conductivity on for temperature distribution of conductive, convective and radiative fin is studied with coefficient of convective heat loss ($N_c = 1$) and coefficient of radiative heat loss $N_r = 2$. Fitness function for given problem can be written as

$$\text{Minimize } \epsilon = \frac{1}{N}\sum_{m=1}^{N}\left(\frac{d^2\theta_m}{dx^2} + \lambda\theta_m\frac{d^2\theta_m}{dx^2} + \lambda\left(\frac{d\theta_m}{dx}\right)^2 - \theta_m - 2\theta_m^4\right)^2 + \frac{1}{2}\left(\left(\frac{d\theta}{dx}(0)\right)^2 + (\theta(1)-1)^2\right), \tag{30}$$

Three cases on bases os dimensionless parameter of thermal conductivity λ are considered to study its effect on tempera-

This article has been accepted for publication in a future issue of this journal, but has not been fully edited. Content may change prior to final publication. Citation information: DOI 10.1109/ACCESS.2021.3117839, IEEE Access

ture distribution of fin.
Case I: Eq (30) with $\lambda = 1.0$.
Case II: Eq (30) with $\lambda = 2.0$.
Case III: Eq (30) with $\lambda = 3.0$.

Problem IV : Effect of Variations in dimensionless parameter of thermal conductivity λ on temperature distribution with $N_c = 1$ and $N_r = 3$.
In this problem, effect on variations in thermal conductivity on temperature distribution of conductive, convective and radiative fins is considered with coefficients of convective heat loss $N_c = 1$ and coefficient of radiative heat loss $N_r = 3$. Fitness based error function for this problem is formulated as

$$\text{Minimize } \epsilon = \frac{1}{N}\sum_{m=1}^{N}\left(\begin{array}{c}\frac{d^2\theta_m}{dx^2} + \lambda\theta_m\frac{d^2\theta_m}{dx^2} + \lambda\left(\frac{d\theta_m}{dx}\right)^2 \\ -\theta_m - 3\theta_m^4\end{array}\right)^2 + \frac{1}{2}\left(\left(\frac{d\theta}{dx}(0)\right)^2 + (\theta(1)-1)^2\right), \tag{31}$$

Following cases on basis of changes in dimensionless parameter of thermal conductivity are considered as follows
Case I: Eq (31) with $\lambda = 1.0$.
Case II: Eq (31) with $\lambda = 2.0$.
Case III: Eq (31) with $\lambda = 3.0$.

VIII. RESULTS AND DISCUSSION

This paper has analyzed the mathematical model for temperature distribution of conductive, convective, and radiative fins with thermal conductivity. The model given by Eq (6) depends on different parameters named as the coefficient of conductive heat loss, coefficient of radiative heat loss, and dimensionless parameter of thermal conductivity. Furthermore, a new soft computing algorithm is designed to study the influence of parameters on temperature distribution of conductive-convective and radiative fins. The behavior of approximate solutions is discussed with trained neurons from [-1,1]. Results obtained by the proposed method are compared with exact solutions, and approximate solution by integration method [71], decomposition method [11], Galerkin method [70] and simplex search method [76].
To study the performance of the proposed technique by obtaining solutions to different cases of each problem, hundred independent simulations have been carried out. Figures 7-14 demonstrates the comparison of best and worst approximate solutions with exact solution along with absolute minimum errors for temperature distribution of each case of problem I, II, III, and IV, respectively. It can be observed from Figure 7 that with neglecting coefficient of radiation and thermal conductivity, temperature distribution of fin decreases and becomes strong convective with increasing coefficient of convection $(N_c = 0.5, 1, 2, 4)$. Furthermore, in the presence of radiation heat loss and thermal conductivity from fin surface we consider $N_r = 1, 2, 3$ and $\lambda = 1, 2, 3$, since these non dimensionless parameters covers most of practical cases [1]. It can be viewed from Figure 9,11 and 13 that with increasing value of thermal conductivity (λ), temperature at fin tip rises and the accuracy of temperature distribution becomes higher. In addition, it can be witnessed that with increasing value of coefficient of convection, the temperature distribution of fin rises with fixed values of thermal conductivity and coefficient of radiation. Plots of best weights obtained by design scheme for calculating temperature distribution of each case of different problem are shown in Figures 15-18. Box plots for fitness evaluation, MAD, TIC, and ENSE are shown in Figures 19-22. It can be seen that mean values of fitness function and performance indicators lies around 10^{-4} to 10^{-6}, 10^{-3} to 10^{-5}, 10^{-4} to 10^{-5} and 10^{-3} to 10^{-6} respectively. The bar graphs are shown in Figures 23-26 represent minimum, mean, median, mode, standard deviation, and variance of fitness value and performance indices obtained by proposed algorithm 100 independent runs.
Approximate solutions obtained by the LeNN-WOA-NM algorithm for different cases of problems I, II, III, and IV are compared with the exact solution and integral method as dictated in Tables 3 and 4. Maximum and minimum absolute errors (AE) of the proposed technique for each case of different problems are given in Tables 5-8. Minimum AE's for case I, II, III and IV of problem I lies between 10^{-11} to 10^{-14}, 10^{-12} to 10^{-14}, 10^{-11} to 10^{-14} and 10^{-9} to 10^{-13} respectively. Minimum AE's for case I, II, and III of problem II lies between 10^{-9} to 10^{-12}, 10^{-10} to 10^{-13} and 10^{-9} to 10^{-11} respectively. Minimum AE's for case I, II and III of problem III lies between 10^{-9} to 10^{-13}, 10^{-10} to 10^{-13} and 10^{-10} to 10^{-12} respectively. Minimum AE's for case I, II and III of problem IV lies between 10^{-9} to 10^{-10}, 10^{-9} to 10^{-12} and 10^{-10} to 10^{-11} respectively. Statistics of fitness value, MAD, TIC, and ENSE in terms of minimum, mean, median, mode, standard deviation and variance are demonstrated through Tables 9-12. It can be seen that the minimum value of fitness function for the problem I, II, III and IV lies around 10^{-13}, 10^{-10}, 10^{-11} and 10^{-10} respectively. Unknown neurons in LeNN structure optimized by design algorithm for obtaining best solutions for temperature distribution of conductive, convective and radiative fins with thermal conductivity. Convergence analysis of the proposed algorithm for each case of problem I-IV is given in Table 17. Statistical results and Figures 27 demonstrates the effectiveness and accuracy of the proposed algorithm.

This article has been accepted for publication in a future issue of this journal, but has not been fully edited. Content may change prior to final publication. Citation information: DOI 10.1109/ACCESS.2021.3117839, IEEE Access

TABLE 3. Comparison between temperature distributions obtained by exact, Integral method and proposed computing technique for different values of N_c with $N_r = \lambda = 0$.

	$N_c = 0.5$			$N_c = 1.0$			$N_c = 2.0$			$N_c = 4.0$		
x	Integral Method	Exact	LeNN-WOA-NM	Integral Method	Exact	LeNN-WOA-NM	Integral Method	Exact	LeNN-WOA-NM	Integral Method	Exact	LeNN-WOA-NM
0.0	0.7931	0.7933	0.7933	0.6471	0.6481	0.6481	0.4545	0.4591	0.4591	0.2500	0.2658	0.2658
0.1	0.7952	0.7953	0.7953	0.6506	0.6513	0.6513	0.4607	0.4637	0.4637	0.2609	0.2711	0.2711
0.2	0.8012	0.8012	0.8012	0.6608	0.6611	0.6611	0.4761	0.4776	0.4776	0.2818	0.2874	0.2874
0.3	0.8113	0.8112	0.8112	0.6776	0.6774	0.6774	0.5011	0.5010	0.5010	0.3138	0.3151	0.3151
0.4	0.8255	0.8252	0.8252	0.7013	0.7006	0.7006	0.5361	0.5345	0.5345	0.3579	0.3555	0.3555
0.5	0.8438	0.8434	0.8434	0.7320	0.7308	0.7308	0.5816	0.5787	0.5787	0.4155	0.4102	0.4102
0.6	0.8663	0.8658	0.8658	0.7699	0.7682	0.7682	0.6384	0.6345	0.6345	0.4884	0.4813	0.4813
0.7	0.8932	0.8925	0.8925	0.8154	0.8134	0.8134	0.7073	0.7030	0.7030	0.5789	0.5717	0.5717
0.8	0.9243	0.9236	0.9236	0.8686	0.8667	0.8667	0.7895	0.7856	0.7856	0.6906	0.6851	0.6851
0.9	0.9599	0.9594	0.9594	0.9300	0.9287	0.9287	0.8864	0.8840	0.8840	0.8245	0.8260	0.8260
1.0	1.0000	1.0000	1.0000	1.0000	1.0000	1.0000	1.0000	0.9999	1.0000	1.0000	0.9999	1.0000

TABLE 4. Comparison between temperature distribution for PROBLEM II, III and IV obtained by proposed algorithm for variations in λ with fixed value of coefficient of convective heat loss ($N_c = 1$).

		$\lambda = 1.0$			$\lambda = 2.0$			$\lambda = 3.0$		
x	N_r	Integral Method	Exact	LeNN-WOA-NM	Integral Method	Exact	LeNN-WOA-NM	Integral Method	Exact	LeNN-WOA-NM
0	1	0.6987	0.7063	0.7063	0.7708	0.7742	0.7742	0.8147	0.8165	0.8165
	2	0.6396	0.6578	0.6578	0.7170	0.7258	0.7258	0.7656	0.7706	0.7706
	3	0.5917	0.6223	0.6223	0.6739	0.6896	0.6896	0.7261	0.7353	0.7353
0.3	1	0.7303	0.7316	0.7316	0.7938	0.7942	0.7942	0.8328	0.8329	0.8329
	2	0.6823	0.6860	0.6860	0.7480	0.7494	0.7494	0.7901	0.7907	0.7907
	3	0.6458	0.6524	0.6524	0.7128	0.7156	0.7156	0.7567	0.7580	0.7580
0.6	1	0.8093	0.8085	0.8085	0.8543	0.8545	0.8545	0.8818	0.8822	0.8822
	2	0.7738	0.7730	0.7730	0.8201	0.8211	0.8211	0.8500	0.8514	0.8514
	3	0.7468	0.7461	0.7461	0.7936	0.7954	0.7954	0.8248	0.8271	0.8271

TABLE 5. Maximum and minimum absolute errors (AE) in solutions of design scheme for cases of Problem I.

	$N_c = 0.5$		$N_c = 1.0$		$N_c = 2.0$		$N_c = 4.0$	
x	Maximum AE	Minimum AE	Maximum AE	Minimum AE	Maximum AE	Minimum AE	Maximum AE	Minimum AE
0.0	1.90E-07	1.20E-11	3.05E-06	1.65E-13	4.25E-07	1.64E-11	1.09E-04	1.52E-10
0.1	1.60E-07	4.32E-11	1.48E-07	2.93E-13	2.32E-06	9.86E-11	4.00E-05	1.15E-09
0.2	1.90E-07	1.70E-12	1.42E-06	3.05E-13	2.53E-09	1.07E-11	8.14E-05	1.79E-10
0.3	1.11E-08	1.70E-11	1.26E-06	6.48E-14	1.50E-06	4.22E-11	1.81E-05	7.65E-10
0.4	6.29E-08	1.84E-11	3.30E-07	7.08E-13	7.45E-07	3.58E-14	5.59E-06	6.84E-13
0.5	1.71E-07	3.91E-14	1.35E-08	2.63E-13	1.70E-07	2.80E-11	4.43E-05	7.46E-10
0.6	8.86E-08	1.58E-11	4.64E-07	2.38E-13	1.78E-06	5.05E-12	3.97E-05	2.32E-10
0.7	1.71E-09	1.67E-11	8.59E-07	1.18E-12	8.46E-07	1.97E-11	1.80E-06	4.98E-10
0.8	1.58E-07	7.41E-13	5.41E-07	5.07E-14	5.56E-07	1.34E-11	2.83E-05	6.87E-10
0.9	1.74E-07	3.44E-11	6.01E-09	2.24E-12	3.66E-06	5.21E-11	5.48E-05	1.19E-09
1.0	1.60E-07	8.13E-12	9.79E-07	3.83E-13	1.62E-06	8.35E-12	2.84E-05	1.01E-10

TABLE 6. Maximum and minimum absolute errors (AE) in solutions of design scheme for cases of Problem II.

	$\lambda = 1.0$		$\lambda = 2.0$		$\lambda = 3.0$	
x	Maximum AE	Minimum AE	Maximum AE	Minimum AE	Maximum AE	Minimum AE
0	9.25E-06	7.25E-11	1.49E-05	3.77E-11	8.97E-06	2.22E-10
0.1	3.39E-05	6.23E-10	1.07E-05	4.45E-10	7.27E-05	2.21E-09
0.2	5.56E-06	1.38E-10	1.41E-05	2.52E-10	2.64E-05	7.38E-10
0.3	1.56E-05	4.69E-10	1.35E-06	1.86E-10	2.46E-05	1.22E-09
0.4	3.28E-05	4.90E-12	3.32E-06	8.06E-11	7.25E-06	9.07E-11
0.5	1.61E-06	6.11E-10	1.18E-05	2.68E-10	2.20E-05	1.40E-09
0.6	2.86E-05	1.89E-10	7.75E-06	5.70E-13	2.96E-07	1.89E-10
0.7	4.93E-05	5.24E-10	4.68E-09	2.55E-10	1.57E-05	1.05E-09
0.8	6.05E-07	8.23E-10	1.05E-05	5.89E-11	3.79E-08	8.89E-10
0.9	1.28E-04	1.54E-09	1.55E-05	3.37E-10	6.46E-06	2.04E-09
1	3.42E-05	1.52E-10	1.17E-05	3.98E-11	1.18E-06	1.89E-10

This article has been accepted for publication in a future issue of this journal, but has not been fully edited. Content may change prior to final publication. Citation information: DOI 10.1109/ACCESS.2021.3117839, IEEE Access

TABLE 7. Maximum and minimum absolute errors (AE) in solutions of design scheme for cases of Problem III.

	$\lambda = 1.0$		$\lambda = 2.0$		$\lambda = 3.0$	
x	Maximum AE	Minimum AE	Maximum AE	Minimum AE	Maximum AE	Minimum AE
0	6.21E-05	4.23E-11	7.48E-06	4.15E-13	3.22E-06	1.51E-11
0.1	3.10E-04	7.68E-10	1.18E-05	1.66E-11	3.89E-06	2.36E-10
0.2	3.04E-11	1.31E-09	1.08E-05	5.75E-11	1.92E-06	3.01E-10
0.3	1.66E-04	1.64E-13	1.53E-07	1.44E-12	8.59E-08	1.39E-11
0.4	8.15E-05	8.40E-10	7.24E-06	6.50E-11	1.61E-06	2.02E-10
0.5	1.63E-05	4.45E-12	1.78E-05	1.03E-13	1.02E-06	2.47E-11
0.6	1.67E-04	6.88E-10	1.03E-05	9.89E-11	2.82E-09	1.62E-10
0.7	7.32E-05	8.13E-12	1.86E-07	9.54E-13	8.29E-07	2.94E-11
0.8	4.81E-05	7.33E-10	2.62E-05	2.00E-10	3.99E-07	2.39E-10
0.9	2.83E-04	2.92E-10	3.92E-05	1.07E-10	3.80E-07	7.10E-11
1	1.18E-04	1.15E-11	3.97E-05	5.45E-12	2.10E-11	2.32E-12

TABLE 8. Maximum and minimum absolute errors (AE) in solutions of design scheme for cases of Problem IV.

	$\lambda = 1.0$		$\lambda = 2.0$		$\lambda = 3.0$	
x	Maximum AE	Minimum AE	Maximum AE	Minimum AE	Maximum AE	Minimum AE
0	3.05E-04	2.15E-09	2.07E-06	1.70E-10	6.55E-05	6.89E-11
0.1	6.96E-05	1.78E-08	5.50E-06	1.90E-09	5.69E-05	4.04E-10
0.2	2.35E-04	4.92E-09	1.23E-06	1.39E-09	7.37E-05	2.42E-11
0.3	1.06E-04	6.84E-09	1.40E-06	3.12E-10	6.95E-06	2.06E-10
0.4	1.74E-07	2.44E-10	4.41E-06	8.83E-10	2.03E-05	8.77E-12
0.5	1.71E-04	5.23E-09	8.71E-07	3.54E-10	7.48E-05	1.18E-10
0.6	1.92E-04	1.55E-09	1.74E-06	6.54E-10	5.45E-05	9.71E-11
0.7	5.36E-05	2.10E-09	6.00E-06	3.30E-10	3.25E-07	4.11E-11
0.8	6.25E-05	6.61E-09	1.89E-07	1.16E-09	7.23E-05	2.05E-10
0.9	3.61E-04	7.90E-09	1.19E-05	2.59E-10	1.27E-04	1.95E-10
1	1.30E-04	5.51E-10	2.16E-06	4.11E-12	9.03E-05	1.23E-11

TABLE 9. Comparison through performance indices for each case of problem I obtained during 100 independent execution of proposed technique.

	Cases	Min	Mean	Median	Mode	Std.	Var.
Fit	$N_c = 0.5$	1.53E-11	3.94E-06	1.08E-07	1.53E-11	2.31E-05	5.36E-10
	$N_c = 1.0$	5.36E-13	3.47E-06	9.79E-08	5.36E-13	1.38E-05	1.91E-10
	$N_c = 2.0$	2.68E-11	3.01E-05	4.79E-07	2.68E-11	2.10E-04	4.40E-08
	$N_c = 4.0$	5.19E-10	1.10E-04	4.97E-06	5.19E-10	6.01E-04	3.61E-07
MAD	$N_c = 0.5$	1.83E-05	5.40E-05	2.79E-05	1.83E-05	1.10E-04	1.21E-08
	$N_c = 1.0$	2.46E-05	5.30E-05	2.95E-05	2.46E-05	8.63E-05	7.44E-09
	$N_c = 2.0$	2.42E-05	1.06E-04	3.00E-05	2.42E-05	3.49E-04	1.22E-07
	$N_c = 4.0$	1.90E-05	2.50E-04	4.55E-05	1.90E-05	9.72E-04	9.45E-07
TIC	$N_c = 0.5$	6.09E-06	1.73E-05	9.22E-06	6.09E-06	3.28E-05	1.07E-09
	$N_c = 1.0$	8.83E-06	1.97E-05	1.07E-05	8.83E-06	3.13E-05	9.78E-10
	$N_c = 2.0$	9.73E-06	4.34E-05	1.34E-05	9.73E-06	1.32E-04	1.74E-08
	$N_c = 4.0$	1.15E-05	1.27E-04	2.53E-05	1.15E-05	4.76E-04	2.26E-07
ENSE	$N_c = 0.5$	8.04E-07	3.57E-05	1.88E-06	8.04E-07	2.67E-04	7.12E-08
	$N_c = 1.0$	5.07E-07	8.50E-06	7.27E-07	5.07E-07	5.00E-05	2.50E-09
	$N_c = 2.0$	2.09E-07	4.72E-05	3.21E-07	2.09E-07	3.74E-04	1.40E-07
	$N_c = 4.0$	7.12E-08	1.98E-04	4.09E-07	7.12E-08	1.75E-03	3.08E-06

This article has been accepted for publication in a future issue of this journal, but has not been fully edited. Content may change prior to final publication. Citation information: DOI 10.1109/ACCESS.2021.3117839, IEEE Access

TABLE 10. Comparison through performance indices for each case of problem II obtained during 100 independent execution of proposed technique.

	Cases	Min	Mean	Median	Mode	Std.	Var.
Fit	$\lambda = 1.0$	4.68E-10	3.18E-05	1.85E-06	4.68E-10	1.16E-04	1.36E-08
	$\lambda = 2.0$	1.78E-10	5.24E-05	1.12E-06	1.78E-10	3.45E-04	1.19E-07
	$\lambda = 3.0$	9.31E-10	2.03E-05	9.69E-07	9.31E-10	1.16E-04	1.34E-08
MAD	$\lambda = 1.0$	1.80E-05	2.12E-04	3.54E-05	1.80E-05	9.61E-04	9.23E-07
	$\lambda = 2.0$	7.62E-06	1.43E-04	2.53E-05	7.62E-06	4.83E-04	2.33E-07
	$\lambda = 3.0$	2.47E-05	8.51E-05	3.23E-05	2.47E-05	2.19E-04	4.79E-08
TIC	$\lambda = 1.0$	6.34E-06	6.39E-05	1.13E-05	6.34E-06	2.83E-04	8.00E-08
	$\lambda = 2.0$	3.25E-06	4.14E-05	8.78E-06	3.25E-06	1.33E-04	1.78E-08
	$\lambda = 3.0$	7.90E-06	2.44E-05	9.87E-06	7.90E-06	5.77E-05	3.33E-09
ENSE	$\lambda = 1.0$	3.87E-07	1.10E-03	1.50E-06	3.87E-07	1.10E-02	1.21E-04
	$\lambda = 2.0$	1.17E-07	5.05E-04	1.29E-06	1.17E-07	4.20E-03	1.74E-05
	$\lambda = 3.0$	1.85E-06	1.66E-04	3.17E-06	1.85E-06	1.10E-03	1.12E-06

TABLE 11. Comparison through performance indices for each case of problem III obtained during 100 independent execution of proposed technique.

	Cases	Min	Mean	Median	Mode	Std.	Var.
Fit	$\lambda = 1.0$	4.27E-10	8.05E-05	6.49E-06	1.63E-07	1.87E-04	3.49E-08
	$\lambda = 2.0$	5.03E-11	8.63E-05	3.94E-06	5.03E-11	4.55E-04	2.07E-07
	$\lambda = 3.0$	1.18E-10	6.17E-05	3.41E-06	1.18E-10	3.11E-04	9.68E-08
MAD	$\lambda = 1.0$	3.16E-05	5.50E-04	6.47E-05	3.23E-05	0.0012	1.55E-06
	$\lambda = 2.0$	1.67E-05	4.87E-04	3.85E-05	1.67E-05	0.0022	4.69E-06
	$\lambda = 3.0$	2.10E-05	1.34E-04	3.97E-05	2.10E-05	3.16E-04	1.00E-07
TIC	$\lambda = 1.0$	1.05E-05	1.70E-04	2.25E-05	1.07E-05	3.79E-04	1.44E-07
	$\lambda = 2.0$	5.62E-06	1.44E-04	1.35E-05	5.62E-06	6.39E-04	4.09E-07
	$\lambda = 3.0$	6.92E-06	3.86E-05	1.23E-05	6.92E-06	8.85E-05	7.84E-09
ENSE	$\lambda = 1.0$	8.86E-07	1.60E-03	3.72E-06	9.24E-07	1.00E-02	9.91E-05
	$\lambda = 2.0$	3.81E-07	6.70E-03	2.03E-06	3.81E-07	5.94E-02	3.50E-03
	$\lambda = 3.0$	8.61E-07	2.28E-04	3.08E-06	8.61E-07	1.40E-03	2.10E-06

TABLE 12. Comparison through performance indices for each case of problem IV obtained during 100 independent execution of proposed technique.

	Cases	Min	Mean	Median	Mode	Std.	Var.
Fit	$\lambda = 1.0$	5.08E-09	3.42E-04	7.17E-05	1.91E-06	5.58E-04	3.11E-07
	$\lambda = 2.0$	6.75E-10	9.65E-05	6.14E-06	6.75E-10	3.40E-04	1.16E-07
	$\lambda = 3.0$	1.26E-10	2.71E-04	4.47E-06	1.26E-10	2.20E-03	4.81E-06
MAD	$\lambda = 1.0$	2.29E-05	0.0023	4.60E-04	2.33E-05	3.80E-03	1.47E-05
	$\lambda = 2.0$	1.88E-05	4.65E-04	5.15E-05	1.88E-05	1.10E-03	1.25E-06
	$\lambda = 3.0$	1.72E-05	6.10E-04	3.44E-05	1.72E-05	2.50E-03	6.05E-06
TIC	$\lambda = 1.0$	8.96E-06	7.33E-04	1.47E-04	9.07E-06	1.20E-03	1.56E-06
	$\lambda = 2.0$	7.48E-06	1.40E-04	1.77E-05	7.48E-06	3.33E-04	1.11E-07
	$\lambda = 3.0$	5.61E-06	1.76E-04	1.10E-05	5.61E-06	7.06E-04	4.99E-07
ENSE	$\lambda = 1.0$	3.86E-07	1.44E-02	1.55E-04	3.99E-07	4.53E-03	2.10E-03
	$\lambda = 2.0$	3.82E-07	1.60E-03	2.85E-06	3.82E-07	6.80E-03	4.60E-05
	$\lambda = 3.0$	4.35E-07	9.40E-03	1.75E-06	4.35E-07	8.25E-03	6.80E-03

This article has been accepted for publication in a future issue of this journal, but has not been fully edited. Content may change prior to final publication. Citation information: DOI 10.1109/ACCESS.2021.3117839, IEEE Access

TABLE 13. Neurons in LeNN structure obtained by proposed technique for different cases of Problem I.

	$N_c = 0.5$			$N_c = 1.0$			$N_c = 2.0$			$N_c = 4.0$		
Index	δ_n	ψ_n	ξ_n	δ_n	ψ_n	ξ_n	δ_n	ψ_n	ξ_n	δ_n	ψ_n	ξ_n
1	-0.0056999	0.56339002	-0.4606574	-0.0814582	1.88462856	-3.3836816	0.22351245	-0.6663826	0.505491167	-0.2122688	-0.41265014	0.020059708
2	-0.9421679	-1.3079032	-0.3347157	-0.0148904	0.70707834	0.41276378	0.47656437	0.69545047	-0.27470296	1.103411242	-0.11144084	-0.01324012
3	0.06428925	0.00505866	-0.3683929	0.57864707	-0.03647	0.06739899	-0.2893142	0.27282928	-0.0116783	-0.37337654	-0.44440324	0.617963109
4	1.05284074	-0.002407	-0.7056344	0.75272266	-0.1936297	-0.0952606	0.03550429	0.42879053	0.448110716	0.695542738	-0.4810622	0.021505784
5	-1.0861276	-0.0099081	0.45922171	0.79960221	0.24060228	-0.0780438	0.60619246	0.00047626	0.422966552	0.85462366	-0.11822472	-0.00887714
6	-0.3813831	0.06902592	0.10915186	-0.3925408	0.06408482	0.09491794	0.71804765	0.29094246	0.077154613	-0.82450308	-0.46530213	-0.05750548
7	2.77693591	-0.3620337	-0.9233865	-1.3871735	-0.3122319	0.02719796	0.83045925	-0.2303568	0.763937695	0.335412263	-0.36612741	0.210247339
8	-0.0004241	-0.0242191	-0.1480398	0.00096331	-0.2407119	-0.6555106	0.14458446	-0.2213035	0.25368457	-0.50587932	-0.20844397	-0.25911716
9	-1.8180972	0.00272134	-0.4997041	0.00816391	-0.01006	0.17454087	0.38877955	0.25946848	0.274271687	0.04196392	-0.07186884	-0.97234379
10	0.74914235	0.14024229	-0.2704175	0.46113581	-0.065251	0.99325379	0.05314317	0.09101029	0.121209977	-0.38475254	0.239319604	-0.60685924
11	0.10657239	0.03889412	0.31447797	0.04506201	0.07960856	0.64450626	0.54268851	-0.0156076	0.375574324	0.09602406	0.018736866	-0.30994201

TABLE 14. Neurons in LeNN structure obtained by proposed technique for different cases of Problem II.

	$\lambda = 1.0$			$\lambda = 2.0$			$\lambda = 3.0$		
Index	δ_n	ψ_n	ξ_n	δ_n	ψ_n	ξ_n	δ_n	ψ_n	ξ_n
1	0.26935844	0.27481814	0.5093007	-0.0569247	-0.0128095	-0.5751289	0.84448022	0.10615057	0.993413424
2	0.98537909	0.82168089	-0.4566929	-0.9198956	-0.4178017	0.01557818	-0.4143321	0.35724283	0.335469194
3	0.30180549	0.30456039	0.00057639	0.04045664	-0.1980751	-0.097936	1.03398222	0.87478855	1.502562163
4	0.07177307	0.34229441	0.32998926	0.47700961	0.03676333	0.68353214	0.0219351	-0.2173315	1.012263325
5	0.33552246	-0.177395	-0.0344335	-0.4022056	-0.3810678	-0.7085721	0.26240062	0.32895515	-0.76232907
6	0.16086163	-0.0819464	0.89464099	0.47690051	-0.345897	0.63588174	0.18557116	-0.4232553	0.54206351
7	-0.0300643	0.3336523	0.01181181	0.05210866	-0.1735951	-0.8706297	-0.0795377	0.07015775	0.902723565
8	0.15173329	0.29932437	0.4069841	-0.6445273	-0.0456398	0.28609717	-0.572535	-0.3785929	0.189610707
9	0.04609494	0.27627505	0.02488004	-0.5862381	0.37941325	-0.4010591	-0.1247952	-0.1615479	0.873108621
10	0.11633037	-0.115249	0.4338842	-0.0069589	-0.0756862	0.4446333	0.08099934	0.24427674	-0.07145994
11	1.07166941	-0.0134561	0.2323527	-0.7844586	-0.1176402	0.5252287	-0.2617872	0.22603824	0.007639225

TABLE 15. Neurons in LeNN structure obtained by proposed technique for different cases of Problem III.

	$\lambda = 1.0$			$\lambda = 2.0$			$\lambda = 3.0$		
Index	δ_n	ψ_n	ξ_n	δ_n	ψ_n	ξ_n	δ_n	ψ_n	ξ_n
1	0.62578938	0.01264802	-0.0314049	1.04065116	0.43626649	-0.5083717	-0.3797966	-0.3102128	0.389930251
2	-0.1167977	0.70370075	-0.5616733	-1.7917414	1.50512181	-1.7462894	-0.2391842	1.01472658	0.380900944
3	0.39160762	-0.9761912	0.00509997	0.1586005	1.08183793	0.46057357	-0.2127764	-0.2546925	1.010985777
4	-0.1872278	-0.3459903	0.12619718	0.04384281	-0.2778872	0.23232805	0.70985312	-0.2274543	-1.02212325
5	0.57380571	-0.307834	-0.4145015	-0.9133443	0.10061135	-0.244175	0.34487281	-0.347361	0.532875028
6	0.57070862	-0.4238162	-0.2190803	-0.7972735	0.20396746	-0.8838576	0.96056849	-0.3200126	0.783810028
7	-0.1313001	-0.3269274	0.45429252	0.35689026	-0.0661261	-0.8422708	-0.0910685	0.18221442	-0.7592668
8	-0.3677613	0.32571374	-0.5598948	1.32054625	0.11131492	-1.2856468	0.58717488	-0.1731806	-0.02173868
9	-0.0054736	0.37042192	0.03862467	-0.0288581	0.09456858	-0.1574551	-0.0013674	0.36693981	0.270824079
10	-0.5487134	0.30053242	0.19205644	-0.289878	-0.4603285	-0.6366003	0.0118006	-0.4410427	0.058796468
11	0.84726777	0.27796037	0.56535073	7.51E-05	-0.2763708	0.39514944	0.00356616	-0.1215339	-0.45959078

This article has been accepted for publication in a future issue of this journal, but has not been fully edited. Content may change prior to final publication. Citation information: DOI 10.1109/ACCESS.2021.3117839, IEEE Access

TABLE 16. Neurons in LeNN structure obtained by proposed technique for different cases of Problem IV.

	$\lambda = 1.0$			$\lambda = 2.0$			$\lambda = 3.0$		
Index	δ_n	ψ_n	ξ_n	δ_n	ψ_n	ξ_n	δ_n	ψ_n	ξ_n
1	0.57174675	1.34289992	0.47516407	0.17752421	-0.0551147	0.59182964	0.13882379	0.13826902	0.203256479
2	0.15215204	0.19122935	0.90103211	0.64405052	1.16139197	-0.0034589	-0.7640621	-0.0236816	-0.00388855
3	0.7133632	0.17390159	-0.5151335	0.15493528	0.81978044	-0.151075	-0.7633091	-0.1350345	-0.88167506
4	0.26577576	0.29965597	-0.6138366	0.003952	0.00967189	0.08888884	-0.866505	0.12627377	0.1918368
5	0.56545429	0.64293736	-0.0712394	0.09809999	0.00216662	0.08226314	0.09815612	-0.0168432	-0.00881928
6	0.38213932	0.28990554	-0.3042828	0.71028955	-0.1888177	0.45684718	0.28417016	0.14442232	-0.02870721
7	0.09838338	0.35454184	-0.1031601	0.22659854	0.47762783	-0.0027904	0.28381553	-0.235924	-0.29817323
8	0.56561309	0.03961569	0.2774475	-0.0395085	0.12463642	0.93020801	0.13726141	-0.7541787	-0.41037637
9	1.81357554	0.33641133	0.27103122	0.02233341	0.77848921	0.00359144	9.40E-05	-0.1211273	-0.73905578
10	0.5177736	0.10448221	-0.6385506	0.00050199	0.97124938	-0.0122281	0.0351829	-0.4556906	-0.07844437
11	0.91392796	0.32060487	0.16558197	-3.06E-06	0.44787914	0.00260238	0.001232	0.02432631	-0.98536794

TABLE 17. Convergence analysis of fitness function and performance measures obtained during 100 independent executions by proposed algorithm.

	Cases	FIT			MAD			TIC			ENSE		
		$\leq 10^{-6}$	$\leq 10^{-7}$	$\leq 10^{-8}$	$\leq 10^{-3}$	$\leq 10^{-4}$	$\leq 10^{-5}$	$\leq 10^{-4}$	$\leq 10^{-5}$	$\leq 10^{-6}$	$\leq 10^{-5}$	$\leq 10^{-6}$	$\leq 10^{-7}$
Problem I	I	98	80	50	100	99	90	100	98	56	98	85	2
	II	93	98	50	100	100	91	100	98	46	99	92	70
	III	87	56	26	100	98	86	99	94	8	96	92	78
	IV	60	35	17	100	98	63	98	75	0	96	79	58
Problem II	I	70	46	22	100	99	68	99	85	46	84	46	68
	II	78	50	29	100	99	75	99	91	56	88	70	46
	III	82	50	31	100	98	90	100	96	52	94	79	0
Problem III	I	52	27	9	100	86	54	95	60	0	60	55	23
	II	62	40	16	100	93	65	98	78	44	73	63	43
	III	69	32	12	100	97	75	100	92	43	87	65	25
Problem IV	I	38	16	3	100	56	0	76	47	10	47	40	18
	II	58	27	8	100	91	61	96	72	36	71	60	48
	III	59	33	18	100	88	62	98	72	48	72	62	45

This article has been accepted for publication in a future issue of this journal, but has not been fully edited. Content may change prior to final publication. Citation information: DOI 10.1109/ACCESS.2021.3117839, IEEE Access

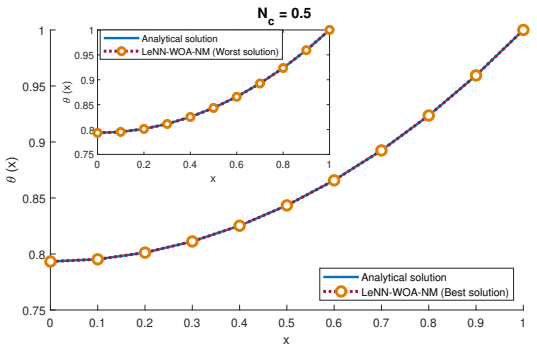

(a) Case I.

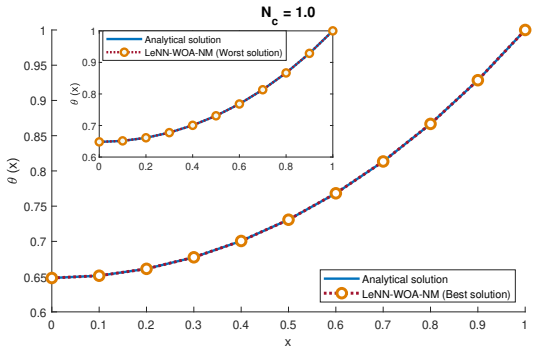

(b) Case II.

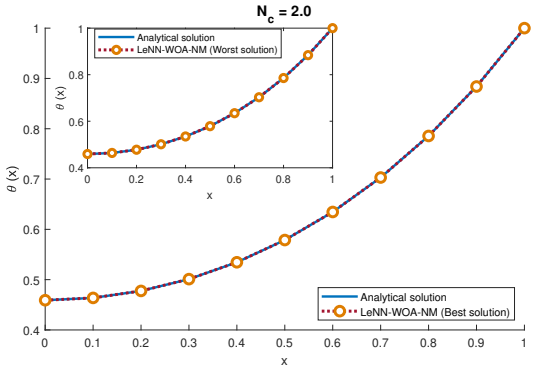

(c) Case III.

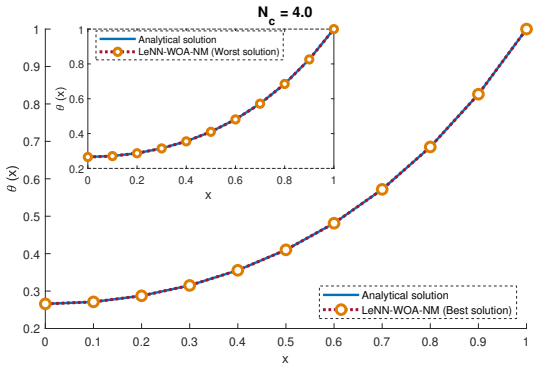

(d) Case IV.

FIGURE 7. Comparison of exact solutions with best and worst solutions obtained by proposed algorithm for problem I.

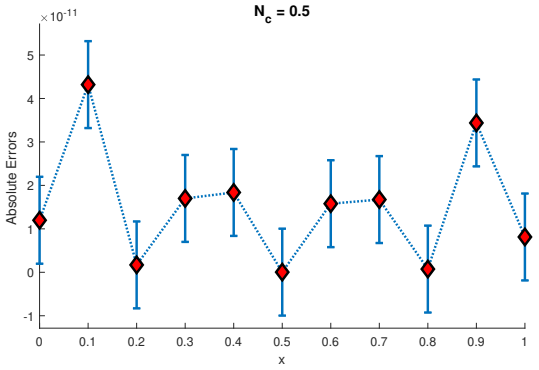

(a) Case I.

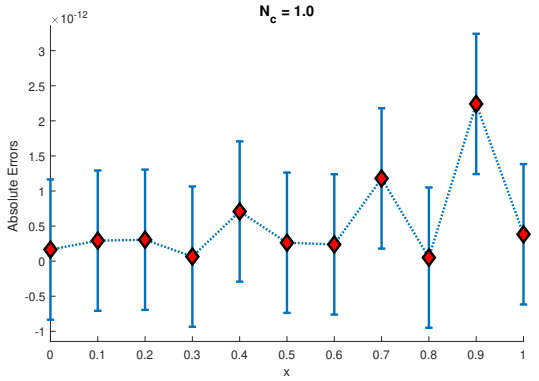

(b) Case II.

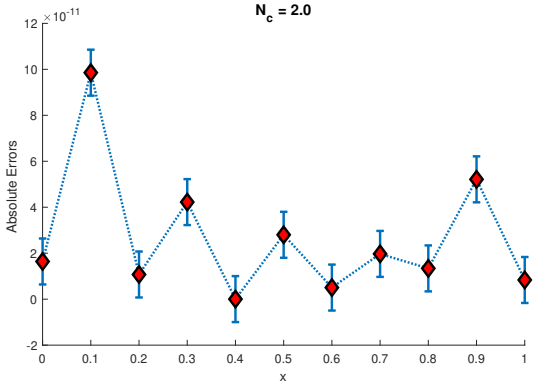

(c) Case III.

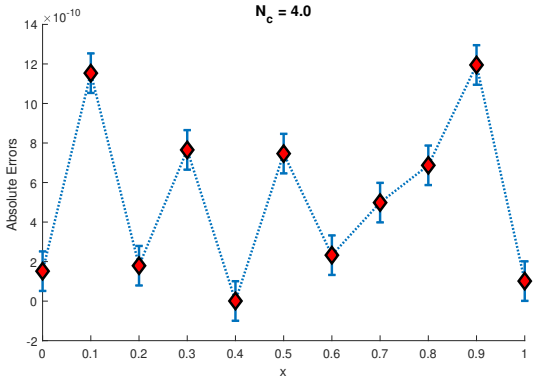

(d) Case IV.

FIGURE 8. Minimum absolute errors (AE) in best solution of proposed technique for each case of Problem I.

This article has been accepted for publication in a future issue of this journal, but has not been fully edited. Content may change prior to final publication. Citation information: DOI 10.1109/ACCESS.2021.3117839, IEEE Access

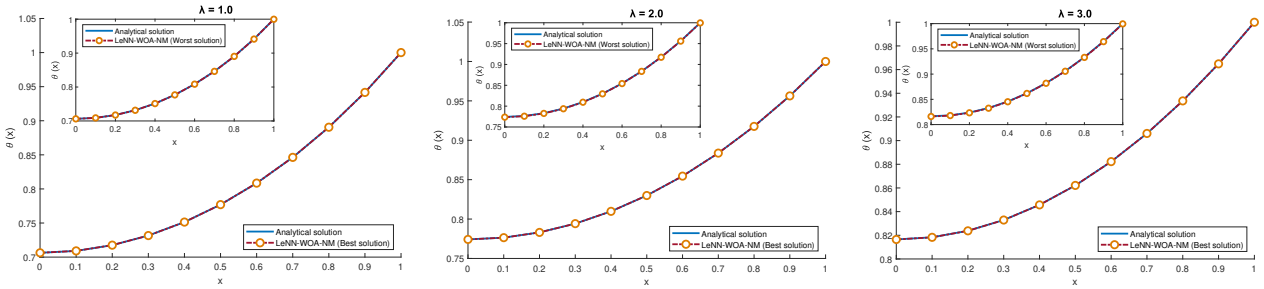

(a) Case I. (b) Case II. (c) Case III.

FIGURE 9. Comparison of exact solutions with best and worst solutions obtained by proposed algorithm for problem II.

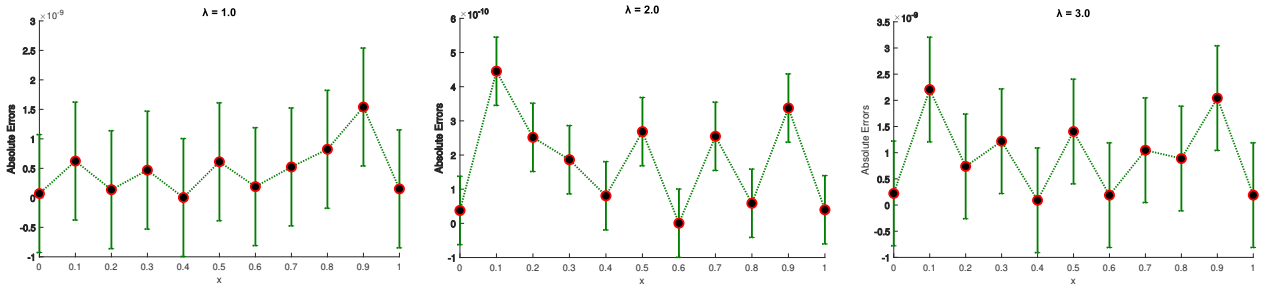

(a) Case I. (b) Case II. (c) Case III.

FIGURE 10. Minimum absolute errors (AE) in best solution of proposed technique for each case of Problem II.

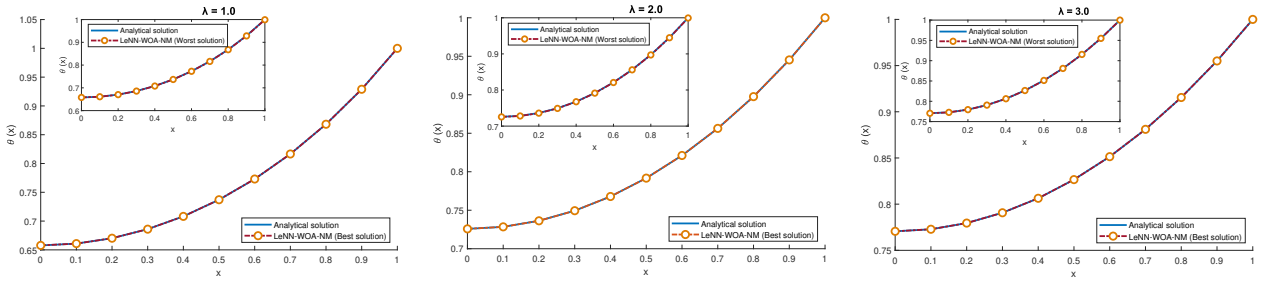

(a) Case I. (b) Case II. (c) Case III.

FIGURE 11. Comparison of exact solutions with best and worst solutions obtained by proposed algorithm for problem III.

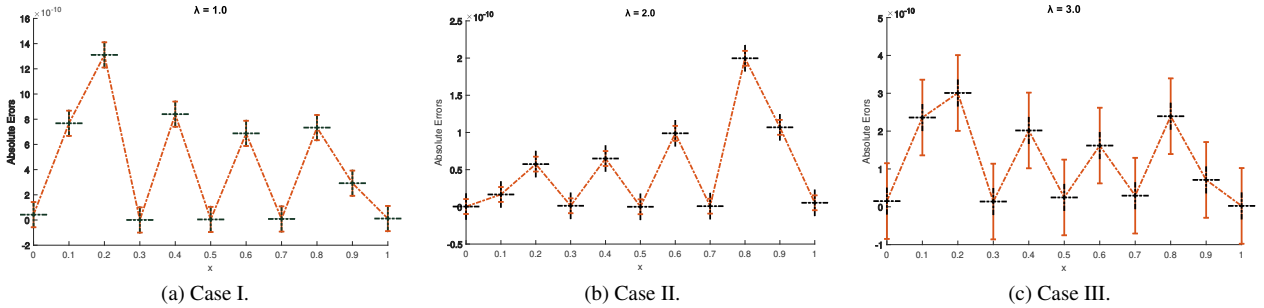

(a) Case I. (b) Case II. (c) Case III.

FIGURE 12. Minimum absolute errors (AE) in best solution of proposed technique for each case of Problem IV.

This article has been accepted for publication in a future issue of this journal, but has not been fully edited. Content may change prior to final publication. Citation information: DOI 10.1109/ACCESS.2021.3117839, IEEE Access

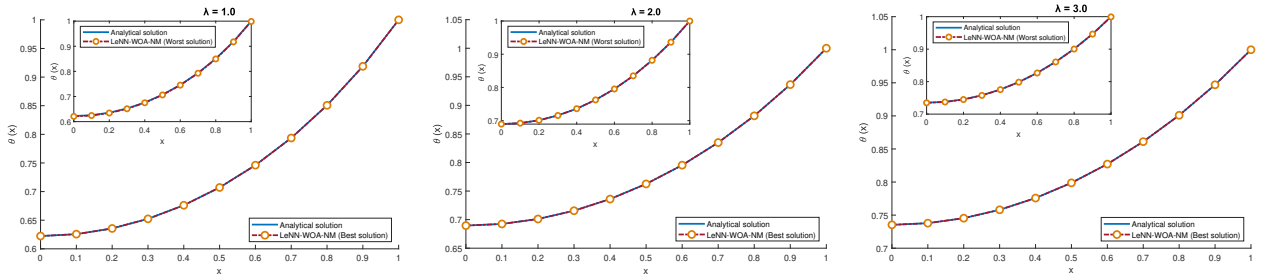

(a) Case I. (b) Case II. (c) Case III.

FIGURE 13. Comparison of exact solutions with best and worst solutions obtained by proposed algorithm for problem IV.

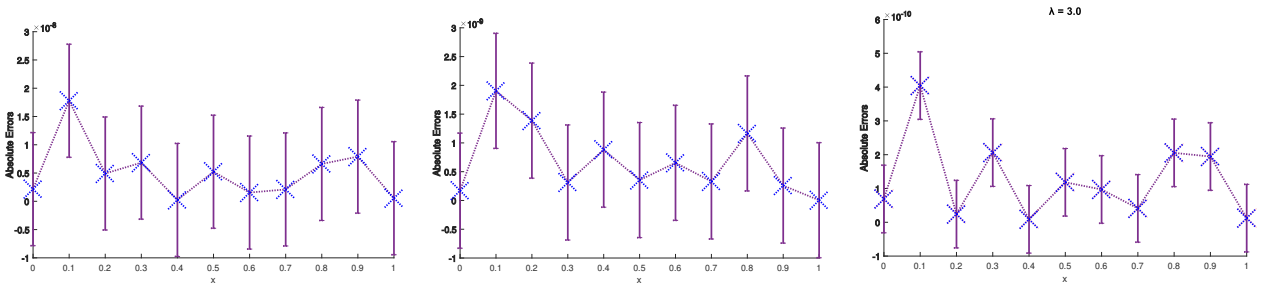

(a) Case I. (b) Case II. (c) Case III.

FIGURE 14. Minimum absolute errors (AE) in best solution of proposed technique for each case of Problem V.

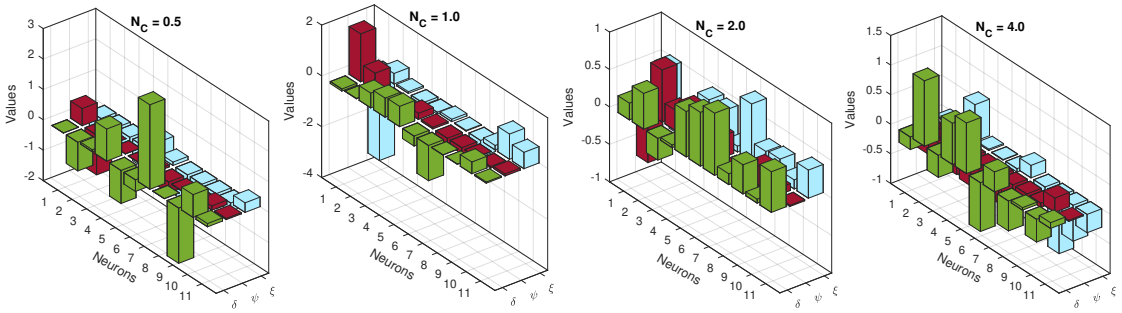

(a) Case I (b) Case II (c) Case III (d) Case IV

FIGURE 15. Trained weights in LeNN optimized by proposed technique for Case I, II, III and IV of problem I.

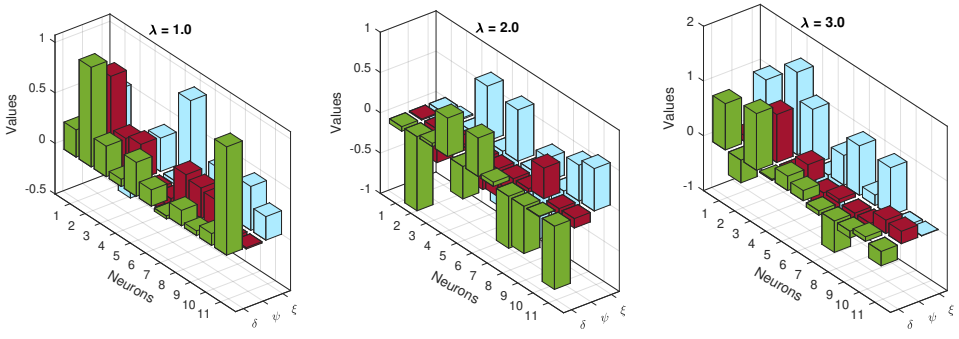

(a) Case I (b) Case II (c) Case III

FIGURE 16. Trained weights in LeNN structure optimized by proposed technique for Case I, II and III of problem II.

This article has been accepted for publication in a future issue of this journal, but has not been fully edited. Content may change prior to final publication. Citation information: DOI 10.1109/ACCESS.2021.3117839, IEEE Access

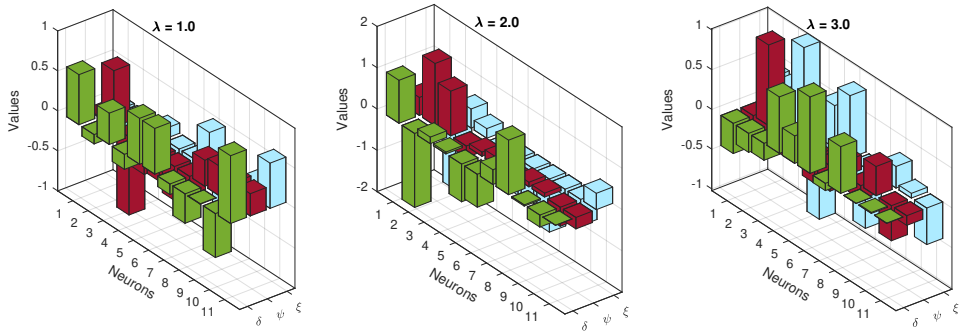

(a) Case I (b) Case II (c) Case III

FIGURE 17. Trained weights in LeNN structure optimized by proposed technique for Case I, II and III of problem III.

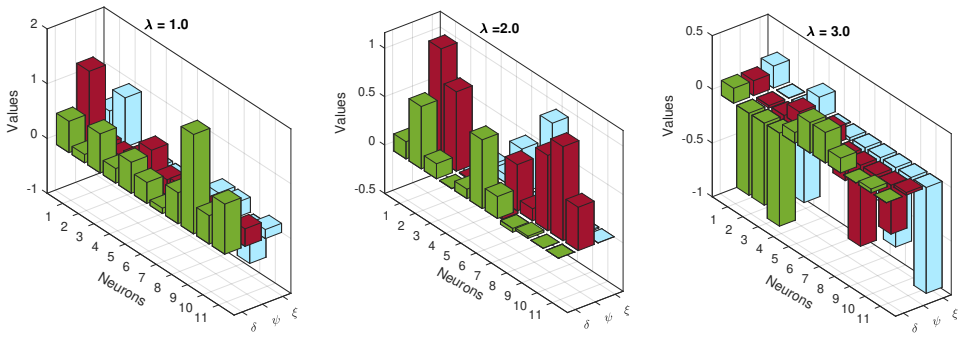

(a) Case I (b) Case II (c) Case III

FIGURE 18. Trained weights in LeNN structure optimized by proposed technique for Case I, II and III of problem IV.

This article has been accepted for publication in a future issue of this journal, but has not been fully edited. Content may change prior to final publication. Citation information: DOI 10.1109/ACCESS.2021.3117839, IEEE Access

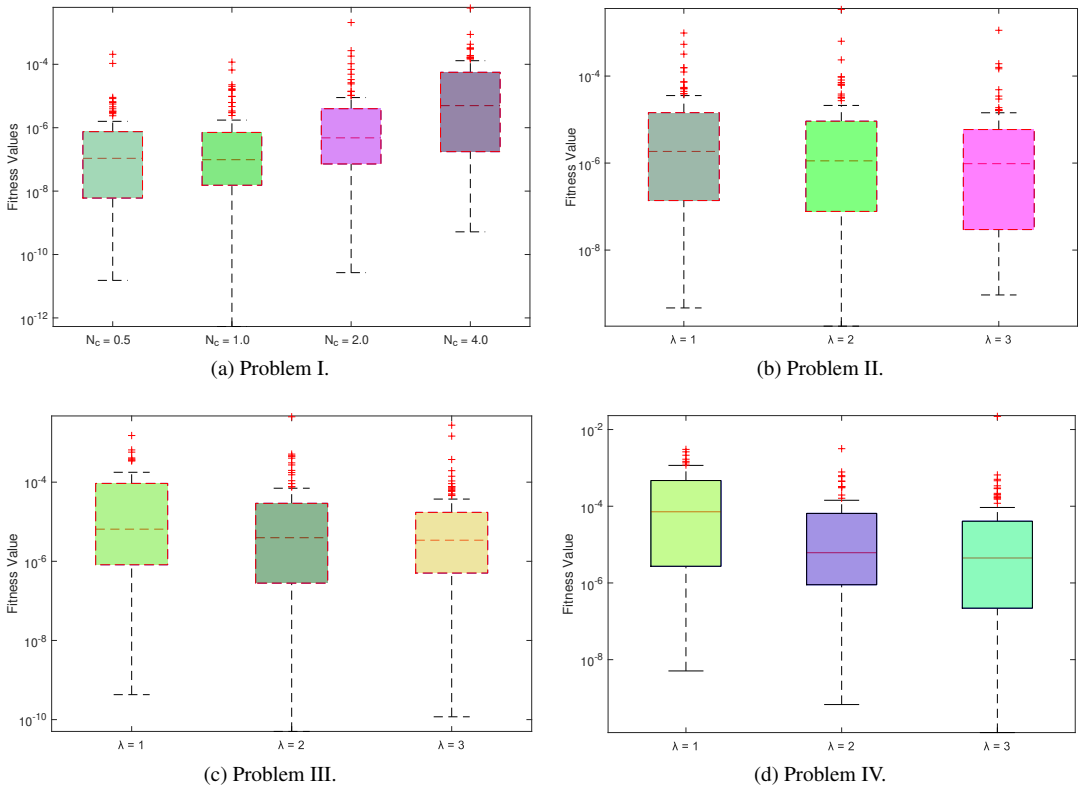

(a) Problem I. (b) Problem II.

(c) Problem III. (d) Problem IV.

FIGURE 19. Box plot for fitness evaluation by proposed algorithm for multiple cases of Problem I-IV.

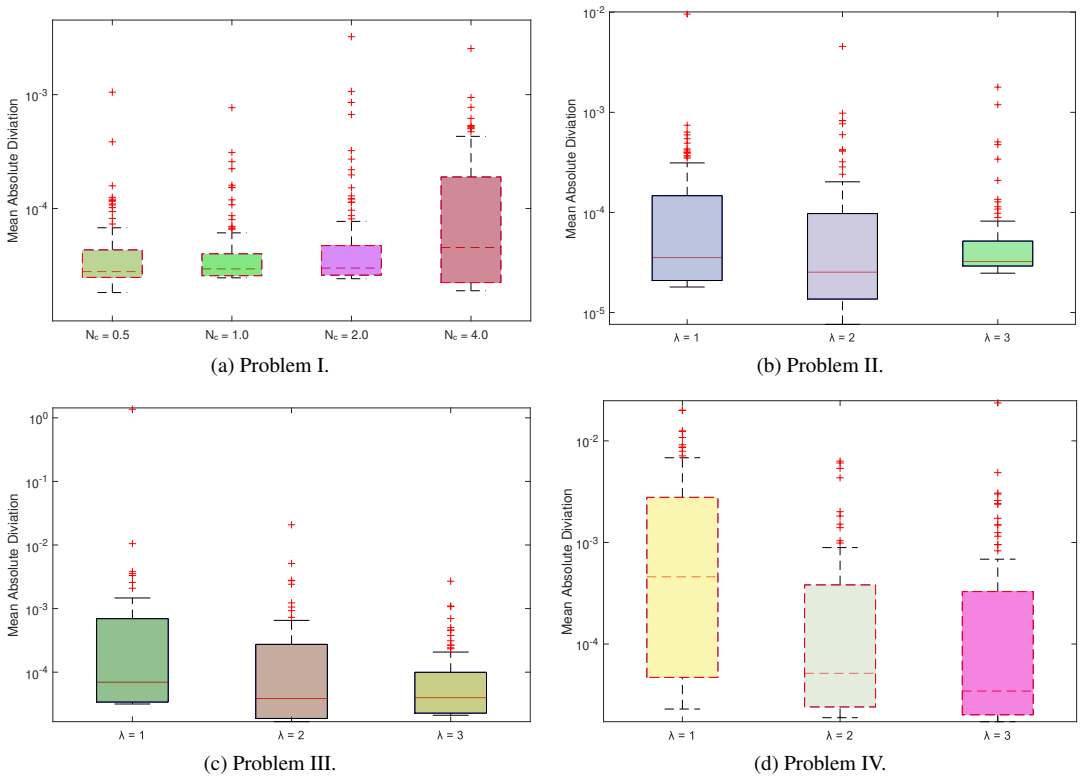

(a) Problem I. (b) Problem II.

(c) Problem III. (d) Problem IV.

FIGURE 20. Box plot for MAD by proposed algorithm for multiple cases of Problem I-IV.

This article has been accepted for publication in a future issue of this journal, but has not been fully edited. Content may change prior to final publication. Citation information: DOI 10.1109/ACCESS.2021.3117839, IEEE Access

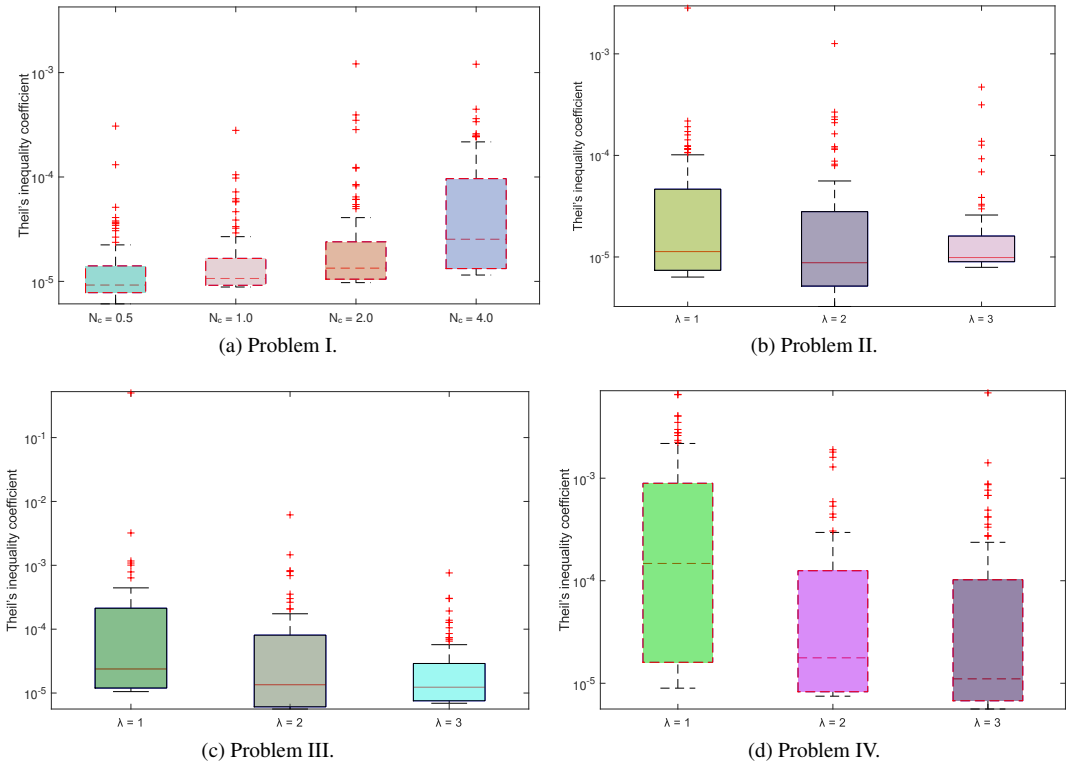

(a) Problem I. (b) Problem II.

(c) Problem III. (d) Problem IV.

FIGURE 21. Box plot for TIC by proposed algorithm for multiple cases of Problem I-IV.

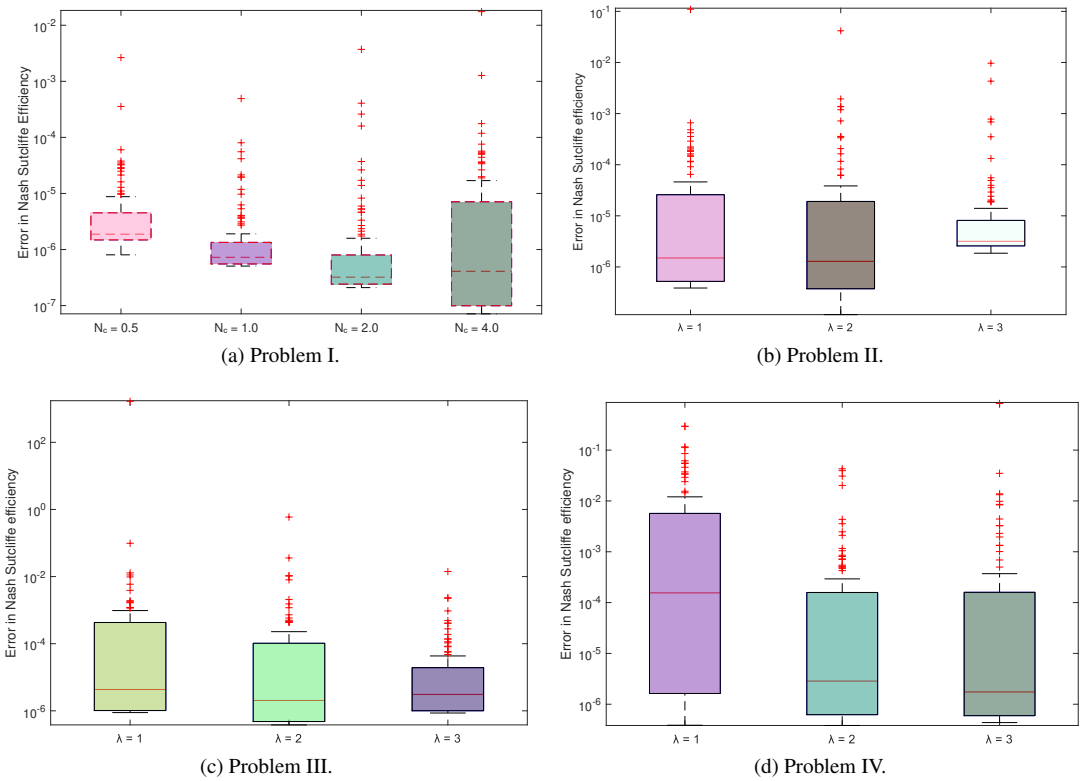

(a) Problem I. (b) Problem II.

(c) Problem III. (d) Problem IV.

FIGURE 22. Box plot for ENSE by proposed algorithm for multiple cases of Problem I-IV.

This article has been accepted for publication in a future issue of this journal, but has not been fully edited. Content may change prior to final publication. Citation information: DOI 10.1109/ACCESS.2021.3117839, IEEE Access

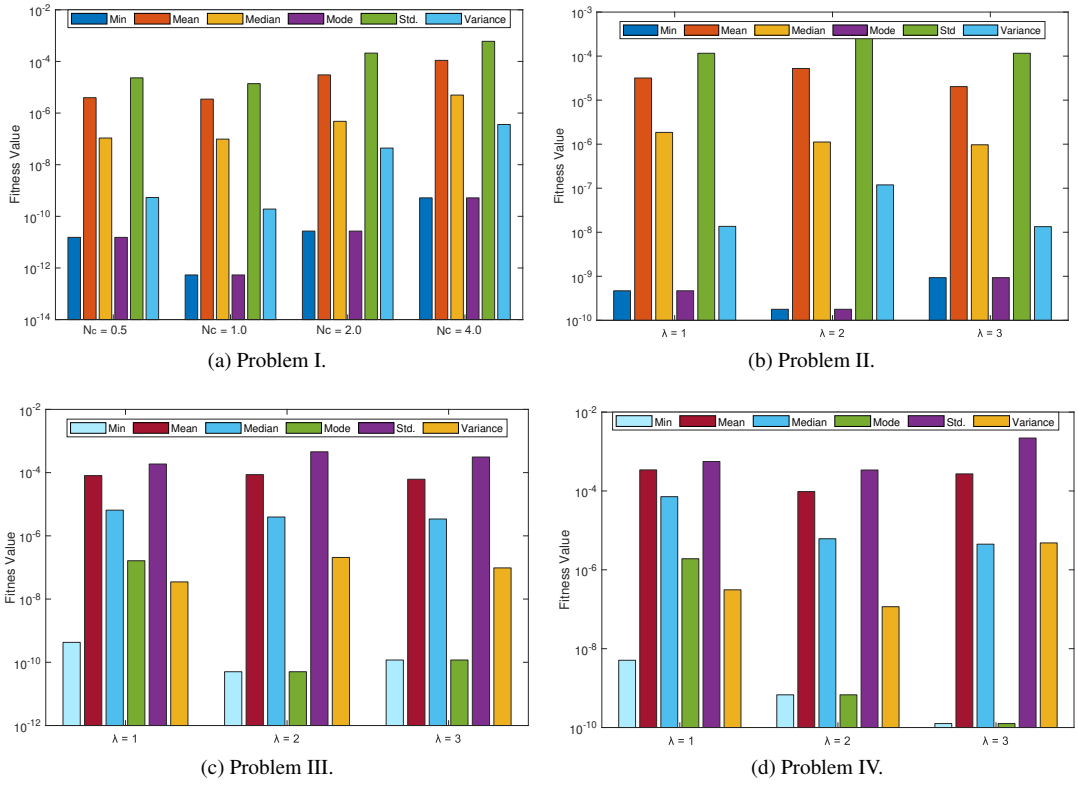

(a) Problem I. (b) Problem II.

(c) Problem III. (d) Problem IV.

FIGURE 23. Performance analysis on fitness value for different cases of Problem I-IV.

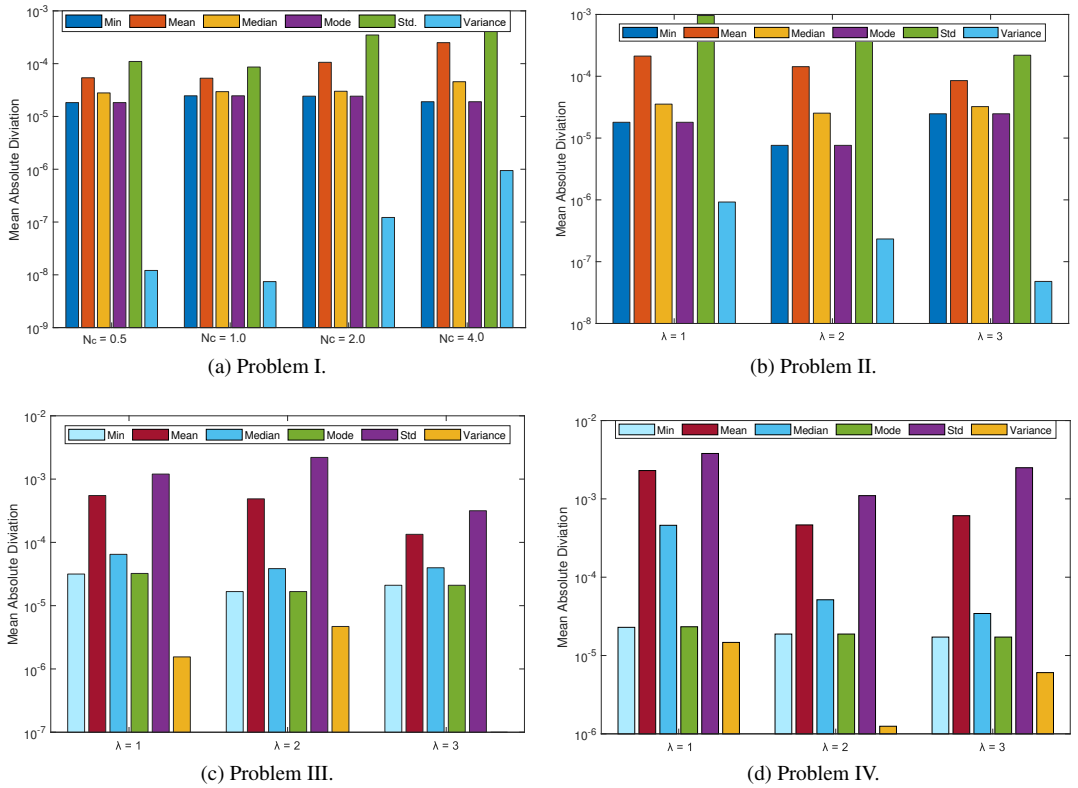

(a) Problem I. (b) Problem II.

(c) Problem III. (d) Problem IV.

FIGURE 24. Performance analysis on MAD for different cases of Problem I-IV.

This article has been accepted for publication in a future issue of this journal, but has not been fully edited. Content may change prior to final publication. Citation information: DOI 10.1109/ACCESS.2021.3117839, IEEE Access

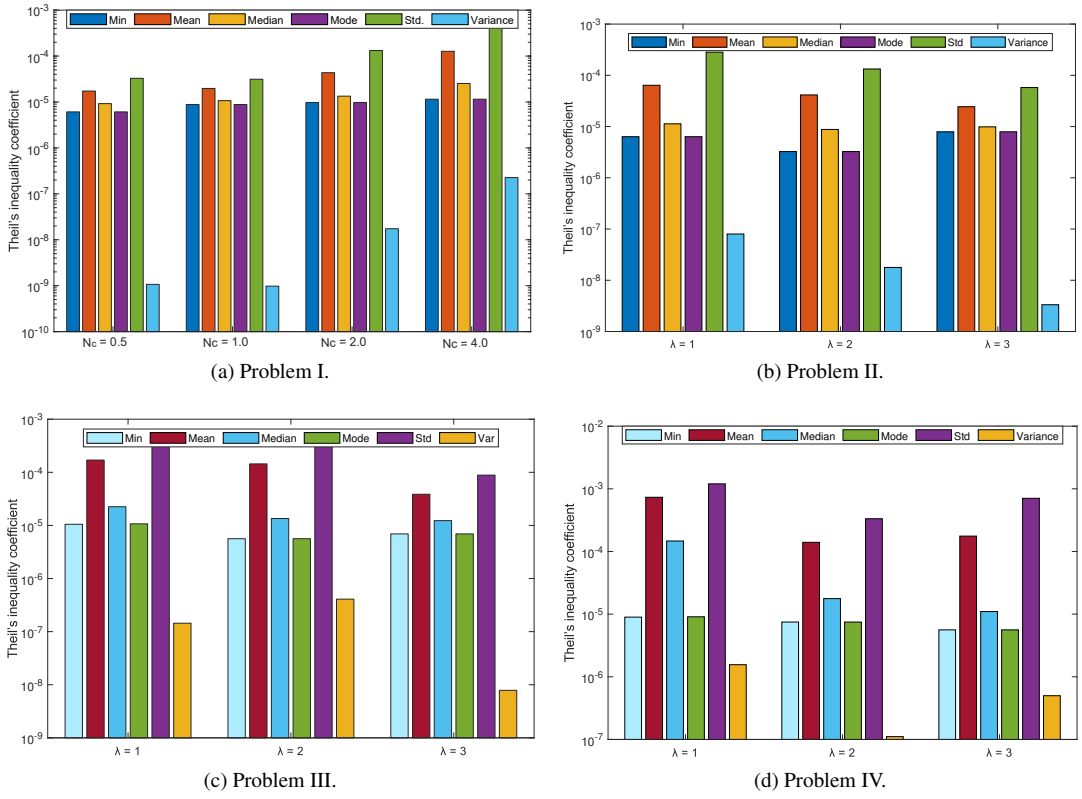

(a) Problem I. (b) Problem II.

(c) Problem III. (d) Problem IV.

FIGURE 25. Performance analysis on TIC for different cases of Problem I-IV.

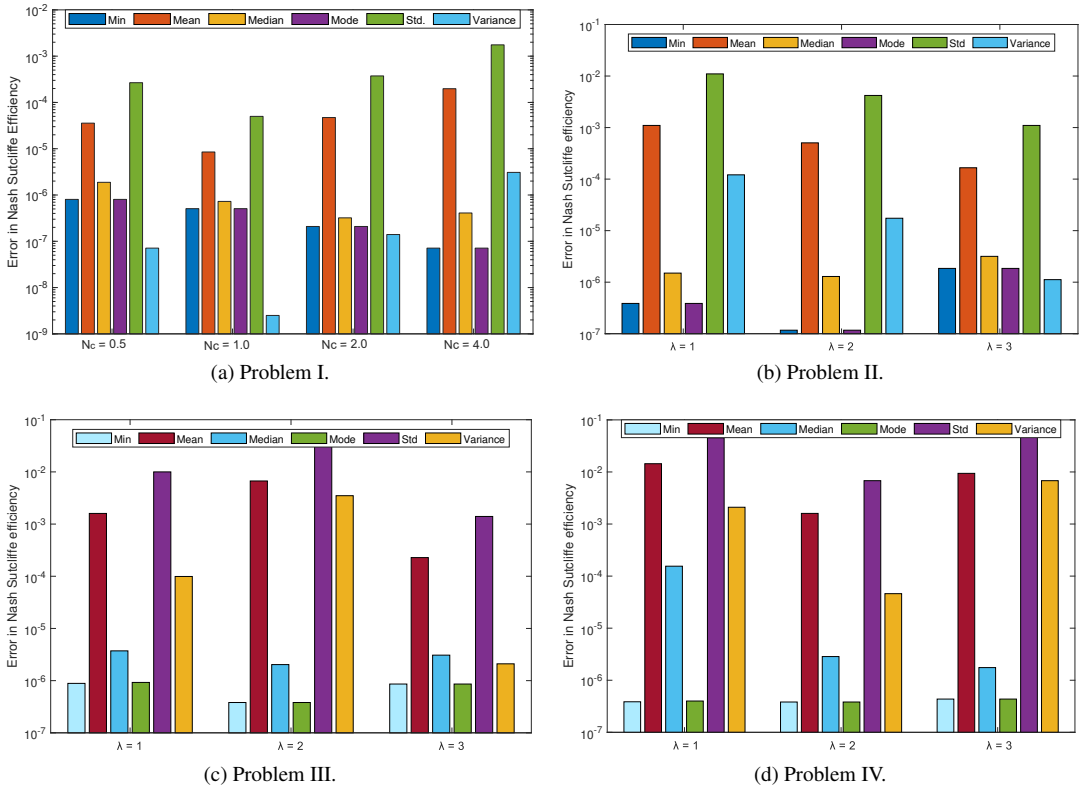

(a) Problem I. (b) Problem II.

(c) Problem III. (d) Problem IV.

FIGURE 26. Performance analysis on ENSE for different cases of Problem I-IV.

This article has been accepted for publication in a future issue of this journal, but has not been fully edited. Content may change prior to final publication. Citation information: DOI 10.1109/ACCESS.2021.3117839, IEEE Access

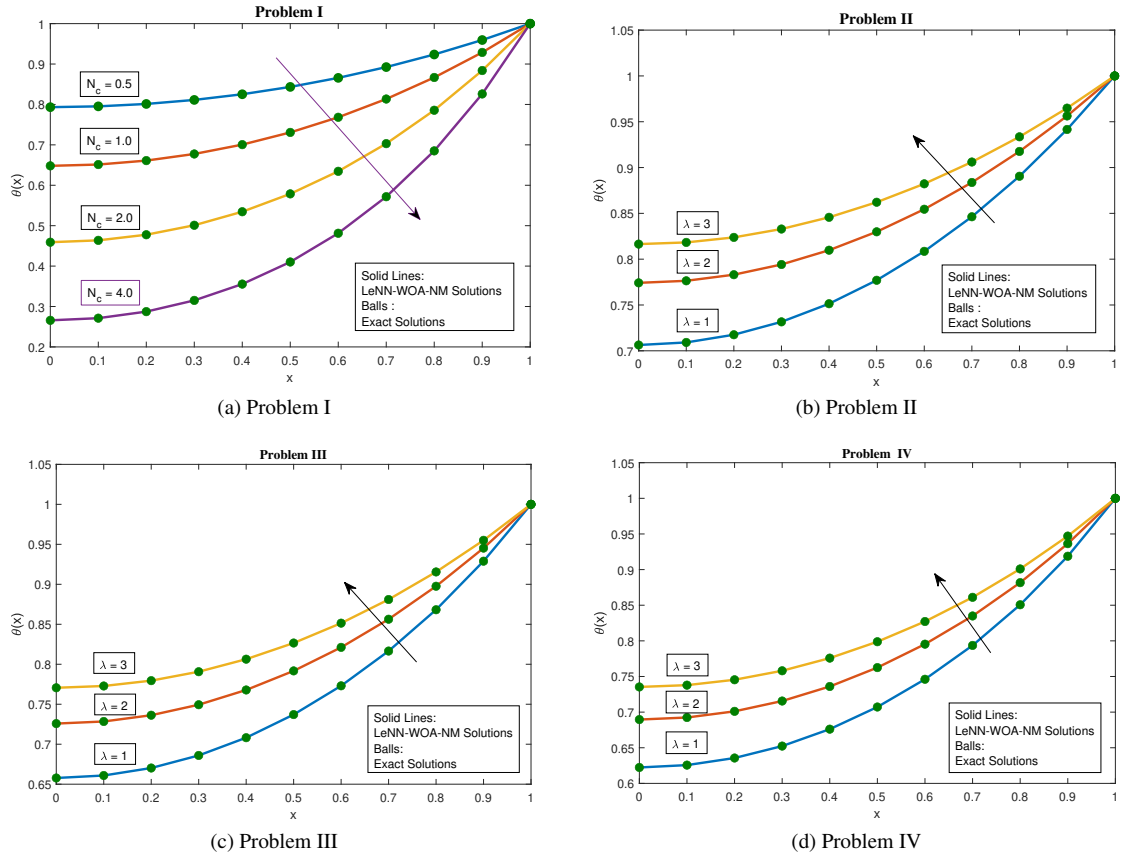

(a) Problem I

(b) Problem II

(c) Problem III

(d) Problem IV

FIGURE 27. Results comparison for temperature distribution obtained by LeNN-WOA-NM algorithm under the influence of N_c, N_r and λ.

This article has been accepted for publication in a future issue of this journal, but has not been fully edited. Content may change prior to final publication. Citation information: DOI 10.1109/ACCESS.2021.3117839, IEEE Access

IX. CONCLUSION

This paper has analyzed a mathematical model for temperature distribution of fin with thermal conductivity in the conductive, convective and radiative environment. Furthermore, we have designed an intelligent soft computing paradigm named as LeNN-WOA-NM algorithm. Weighted Legendre polynomials are used to model approximate series solutions for temperature distribution under the influence of variations in thermal conductivity (λ) and coefficients of convective and radiative heat loss N_c and N_r. We summarize our findings as follows:

- In problem I, with the increasing value of the coefficient of convective heat loss, the excess of temperature is getting lower, which decreases the transfer of heat and fin becomes strong convective as shown in Figure 27(a).
- With the increasing value of dimensionless parameter λ in thermal conductivity, the excess of temperature becomes higher, and the transfer of heat increases. Figure 27(b),(c) and (d) represent the behavior of temperature distribution for problem II, III and IV, respectively.
- Approximate solutions obtained by LeNN-WOA-NM algorithm are compared with exact solutions, and integral methods [71]. Tables 21-25 shows the accuracy of proposed technique in obtaining solutions for temperature distributions under influence of N_c,N_r and λ.
- Minimum absolute errors in approximate solutions by design algorithm prove that LeNN-WOA-NM is efficient and accurate. Moreover, the values of performance indicators MAD, TIC and ENSE extend the worth of the designed scheme.
- Convergence of proposed algorithm has been proven by boxplots and bar graphs representing the minimum and mean values of performance indicators obtained during 100 independent runs.
- From the above-discussed figures and tables, it should be noted that the lower value of convection and radiation parameter, the higher is the accuracy of approximate solutions, while larger the value of thermal conductivity, the more accurate the approximate temperature distributions for fins.

In the future, the application of Legendre neural networks-based soft computing algorithms can be extended to solve highly nonlinear and stiff models arising in different applications of practical interest.

X. APPENDIX

Approximate solution obtained by proposed algorithm for problem I with $N_c = 0.5, 1.0, 2.0$ and 4.0 are given as

$$\begin{aligned}
\theta_{approx}(x) &= -0.0056999 + (-0.9421679x - 1.3079032)(-0.3347157) \\
&+ \left(\frac{3(0.06428925x + 0.00505866)^2 - 1}{2}\right)(-0.3683929) \\
&+ \left(\frac{5(1.052841x - 0.00241)^3 - 3(1.052841x - 0.00241)}{2}\right)(-0.70563) \\
&+ \left(\frac{35(-1.086128x - 0.009908)^4 - 30(-1.086128x - 0.009908)^2}{8} + \frac{3}{8}\right)(0.459222) \\
&+ \left(\frac{63(-0.3813831x+0.06902592)^5 - 70(-0.3813831x+0.06902592)^3}{8} + \frac{15(-0.3813831x+0.06902592)}{8}\right)(0.10915186) \\
&+ \left(\frac{231(2.77693591x-0.3620337)^6 - 315(2.77693591x-0.3620337)^4}{16} + \frac{105(2.77693591x-0.3620337)^2 - 5}{16}\right)(-0.9233865) \\
&+ \left(\frac{429(-0.0004241x-0.0242191)^7 - 693(-0.0004241x-0.0242191)^5}{16} + \frac{315(-0.0004241x-0.0242191)^2 - 35(-0.0004241x-0.0242191)}{16}\right)(-0.148039) \\
&+ \left(\frac{6435(-1.81809x+0.002721)^8 - 12012(-1.81809x+0.002721)^6}{128} + \frac{6930(-1.81809x+0.002721)^4 - 1260(-1.81809x+0.002721)^2 + 35)}{128}\right)(-0.49971). \\
&+ \left(\frac{12155(0.749142x+0.140242)^9 - 25740(0.749142x+0.140242)^7}{128} + \frac{+18018(0.749142x+0.140242)^5 - 4620(0.749142x+0.140242)^3}{128} + \frac{+315(0.749142x+0.140242)}{128}\right)(-0.2704175) \\
&+ \left(\frac{46189(0.106572x+0.038894)^{10} - 109395(0.106572x+0.03889)^8}{256} + \frac{+90090(0.106572x+0.038894)^6 - 30030(0.10657239x+0.03889)^4}{128} + \frac{+3465(0.106572x+0.03889)^2 - 63}{128}\right)(0.31448)
\end{aligned}$$

$$\begin{aligned}
\theta_{approx}(x) &= -0.0814582 + (-0.0148904x + 0.70707834)(0.41276378) \\
&+ \left(\frac{3(0.57864707x - 0.03647)^2 - 1}{2}\right)(0.06739899) \\
&+ \left(\frac{5(0.75272266x - 0.1936297)^3 - 3(0.75272266x - 0.1936297)}{2}\right)(-0.0952606) \\
&+ \left(\frac{35(0.79960x + 0.240602)^4 - 30(0.79960x + 0.240602)^2}{8} + \frac{3}{8}\right)(-0.078044) \\
&+ \left(\frac{63(-0.39254x+0.064085)^5 - 70(-0.39254x+0.064085)^3}{8} + \frac{15(-0.39254x+0.064085)}{8}\right)(0.0949179) \\
&+ \left(\frac{231(-1.38717x-0.31223)^6 - 315(-1.38717x-0.31223)^4}{16} + \frac{105(-1.38717x-0.31223)^2 - 5}{16}\right)(0.02719) \\
&+ \left(\frac{429(0.00096x-0.24071)^7 - 693(0.00096x-0.24071)^5}{16} + \frac{315(0.00096x-0.24071)^2 - 35(0.00096x-0.24071)}{16}\right)(-0.65551) \\
&+ \left(\frac{6435(0.008164x-0.0101)^8 - 12012(0.008164x-0.0101)^6}{128} + \frac{6930(0.008164x-0.0101)^4 - 1260(0.008164x-0.0101)^2 + 35)}{128}\right)(0.174541). \\
&+ \left(\frac{12155(0.46114x-0.06525)^9 - 25740(0.46114x-0.06525)^7}{128} + \frac{+18018(0.46114x-0.06525)^5 - 4620(0.46114x-0.06525)^3}{128} + \frac{+315(0.46114x-0.06525)}{128}\right)(0.993254) \\
&+ \left(\frac{46189(0.04506x+0.079609)^{10} - 109395(0.04506x+0.079609)^8}{256} + \frac{+90090(0.04506x+0.079609)^6 - 30030(0.04506x+0.079609)^4}{128} + \frac{+3465(0.04506x+0.079609)^2 - 63}{128}\right)(0.64451)
\end{aligned}$$

This article has been accepted for publication in a future issue of this journal, but has not been fully edited. Content may change prior to final publication. Citation information: DOI 10.1109/ACCESS.2021.3117839, IEEE Access

Nomenclature

Abbreviation	Description	Abbreviation	Description
LeNN	Legendre Neural Networks	α	Reflection Coefficient
NM	Nelder-Mead Algorithm	β	Expansion Coefficient
MAD	Mean Absolute Deviation	γ	Contraction Coefficient
TIC	Theil's inequality coefficient	δ	Shrink Coefficient.
NSE	Nash Sutcliffe Efficiency	L	Axial length,
ENSE	Error In Nash Sutcliffe Efficiency	T_b	Base temperature,
λ	Dimensionless constant in the thermal conductivity	ϵ	Surface emissivity,
x	Dimensionless axial distance measured from the tip	T_s	Sink temperature
X	Axial distance measured from the fin's tip	T_a	Ambient temperature,
p	Random number	b, l	Arbitrary constants
$X*$	Best solution of WOA so far	A	Cross section
N_c	Coefficient of convective heat loss	x^e	Expansion point in NM
N_r	Coefficient of radiative heat loss	$\vec{A}, \vec{C}$	Coefficient vectors
x^0	Centroid value	x^r	Reflection point
x^h	Worst value	x^b	Best value

$$\theta_{approx}(x) = 0.22351245 + (0.47656437x + 0.69545047)(-0.27470296)$$
$$+\left(\frac{3(-0.2893142x + 0.27282928)^2 - 1}{2}\right)(-0.0116783)$$
$$+\left(\frac{5(0.035504x + 0.4287905)^3 - 3(0.035504x + 0.428791)}{2}\right)(0.448111)$$
$$+\left(\frac{35(0.606193x + 0.000476)^4 - 30(0.606193x + 0.000476)^2}{8} + \frac{3}{8}\right)(0.42297)$$
$$+\left(\frac{63(0.71805x+0.290943)^5-70(0.71805x+0.290943)^3}{8} + \frac{15(0.71805x+0.290943)}{8}\right)(0.42297)$$
$$+\left(\frac{231(0.83046x-0.23036)^6-315(0.83046x-0.23036)^4}{16} + \frac{105(0.83046x-0.23036)^2-5}{16}\right)(0.76394)$$
$$+\left(\frac{429(0.14459x-0.2213)^7-693(0.14459x-0.2213)^5}{16} + \frac{315(0.14459x-0.2213)^2-35(0.14459x-0.2213)}{16}\right)(0.25369)$$
$$+\left(\frac{6435(0.3888x+0.25947)^8-12012(0.3888x+0.25947)^6}{128} + \frac{6930(0.3888x+0.25947)^4-1260(0.3888x+0.25947)^2+35)}{128}\right)(0.274272).$$
$$+\left(\frac{12155(0.05314x+0.09101)^9-25740(0.05314x+0.09101)^7}{128} + \frac{+18018(0.05314x+0.09101)^5-4620(0.05314x+0.09101)^3}{128} + \frac{+315(0.05314x+0.09101)}{128}\right)(0.121209)$$
$$+\left(\frac{46189(0.54269x-0.015608)^{10}-109395(0.54269x-0.015608)^8}{256} + \frac{+90090(0.54269x-0.015608)^6-30030(0.54269x-0.015608)^4}{128} + \frac{+3465(0.54269x-0.015608)^2-63}{128}\right)(0.37557)$$

$$\theta_{approx}(x) = -0.2122688 + (1.103411242x - 0.11144084)(-0.01324012)$$
$$+\left(\frac{3(-0.37337654x - 0.44440324)^2 - 1}{2}\right)(0.617963109)$$
$$+\left(\frac{5(0.69554274x - 0.481062)^3 - 3(0.69554274x - 0.481062)}{2}\right)(0.0215058)$$
$$+\left(\frac{35(0.854624x - 0.118225)^4 - 30(0.854624x - 0.118225)^2}{8} + \frac{3}{8}\right)(-0.00888)$$
$$+\left(\frac{63(-0.8245x-0.4653)^5-70(-0.8245x-0.4653)^3}{8} + \frac{15(-0.8245x-0.4653)}{8}\right)(-0.0575)$$
$$+\left(\frac{231(0.3354x-0.36613)^6-315(0.3354x-0.36613)^4}{16} + \frac{105(0.3354x-0.36613)^2-5}{16}\right)(0.21025)$$
$$+\left(\frac{429(-0.5059x-0.2084)^7-693(-0.5059x-0.2084)^5}{16} + \frac{315(-0.5059x-0.2084)^2-35(-0.5059x-0.2084)}{16}\right)(-0.25912)$$
$$+\left(\frac{6435(0.04196x-0.07187)^8-12012(0.04196x-0.07187)^6}{128} + \frac{6930(0.04196x-0.07187)^4-1260(0.04196x-0.07187)^2+35)}{128}\right)(-0.9723).$$
$$+\left(\frac{12155(-0.3848x+0.23932)^9-25740(-0.3848x+0.23932)^7}{128} + \frac{+18018(-0.3848x+0.23932)^5-4620(-0.3848x+0.23932)^3}{128} + \frac{+315(-0.3848x+0.23932)}{128}\right)(-0.60686)$$
$$+\left(\frac{46189(0.09602x+0.018737)^{10}-109395(0.09602x+0.018737)^8}{256} + \frac{+90090(0.09602x+0.018737)^6-30030(0.09602x+0.018737)^4}{128} + \frac{+3465(0.09602x+0.018737)^2-63}{128}\right)(-0.3099)$$

Approximate solution obtained by proposed algorithm for

This article has been accepted for publication in a future issue of this journal, but has not been fully edited. Content may change prior to final publication. Citation information: DOI 10.1109/ACCESS.2021.3117839, IEEE Access

problem II with $\lambda = 1.0, 2.0$ and 3.0 are given as

$$\begin{aligned}\theta_{approx}(x) &= 0.26935844 + (0.98537909x + 0.82168089)(-0.4566929)\\ &+\left(\frac{3(0.30180549x+0.30456039)^2-1}{2}\right)(0.00057639)\\ &+\left(\frac{5(0.071773x+0.342294)^3-3(0.071773x+0.342294)}{2}\right)(0.329989)\\ &+\left(\frac{35(0.33552x-0.177395)^4-30(0.33552x-0.177395)^2}{8}+\frac{3}{8}\right)(-0.0344)\\ &+\left(\frac{63(0.16086x-0.08195)^5-70(0.16086x-0.08195)^3}{8}+\frac{15(0.16086x-0.08195)}{8}\right)(0.8946)\\ &+\left(\frac{231(-0.03006x+0.3337)^6-315(-0.03006x+0.3337)^4}{16}+\frac{105(-0.03006x+0.3337)^2-5}{16}\right)(0.01181)\\ &+\left(\frac{429(0.15173x+0.2993)^7-693(0.15173x+0.2993)^5}{16}+\frac{315(0.15173x+0.2993)^2-35(0.15173x+0.2993)}{16}\right)(0.40698)\\ &+\left(\frac{6435(0.04196x-0.07187)^8-12012(0.04196x-0.07187)^6}{128}+\frac{6930(0.04196x-0.07187)^4-1260(0.04196x-0.07187)^2+35)}{128}\right)(0.02488).\\ &+\left(\frac{12155(0.0461x+0.27626)^9-25740(0.0461x+0.27626)^7}{128}+\frac{18018(0.0461x+0.27626)^5-4620(0.0461x+0.27626)^3}{128}+\frac{315(0.0461x+0.27626)}{128}\right)(0.43388)\\ &+\left(\frac{46189(1.0717x-0.01347)^{10}-109395(1.0717x-0.013477)^8}{256}+\frac{90090(0.09602x+0.018737)^6-30030(1.0717x-0.01347)^4}{128}+\frac{3465(1.0717x-0.01347)^2-63}{128}\right)(0.23235)\end{aligned}$$

$$\begin{aligned}\theta_{approx}(x) &= 0.84448022 + (-0.4143321x + 0.35724283)(0.335469194)\\ &+\left(\frac{3(1.03398222x+0.87478855)^2-1}{2}\right)(1.502562163)\\ &+\left(\frac{5(0.02193x-0.21733)^3-3(0.02193x-0.21733)}{2}\right)(1.01226)\\ &+\left(\frac{35(0.2624x+0.32896)^4-30(0.2624x+0.32896)^2}{8}+\frac{3}{8}\right)(-0.762329)\\ &+\left(\frac{63(0.18557x-0.4233)^5-70(0.18557x-0.4233)^3}{8}+\frac{15(0.18557x-0.4233)}{8}\right)(0.5421)\\ &+\left(\frac{231(-0.07954x+0.07016)^6-315(-0.07954x+0.07016)^4}{16}+\frac{105(-0.07954x+0.07016)^2-5}{16}\right)(0.90272)\\ &+\left(\frac{429(-0.5725x-0.37859)^7-693(-0.5725x-0.37859)^5}{16}+\frac{315(-0.5725x-0.37859)^2-35(-0.5725x-0.37859)}{16}\right)(0.1896)\\ &+\left(\frac{6435(-0.1248x-0.16155)^8-12012(-0.1248x-0.16155)^6}{128}+\frac{6930(-0.1248x-0.16155)^4-1260(-0.1248x-0.16155)^2+35)}{128}\right)(0.87311).\\ &+\left(\frac{12155(0.08099x+0.24428)^9-25740(0.08099x+0.24428)^7}{128}+\frac{18018(0.08099x+0.24428)^5-4620(0.08099x+0.24428)^3}{128}+\frac{315(0.08099x+0.24428)}{128}\right)(-0.07146)\\ &+\left(\frac{46189(-0.2618x+0.22604)^{10}-109395(-0.2618x+0.22604^8}{256}+\frac{90090(-0.2618x+0.22604)^6-30030(-0.2618x+0.22604)^4}{128}+\frac{3465(-0.2618x+0.22604)^2-63}{128}\right)(0.00764)\end{aligned}$$

Approximate solution obtained by proposed algorithm for problem III with $\lambda = 1.0, 2.0$ and 3.0 are given as

$$\begin{aligned}\theta_{approx}(x) &= -0.0569247 + (-0.9198956x - 0.4178017)(0.01557818)\\ &+\left(\frac{3(0.04045664x-0.1980751)^2-1}{2}\right)(-0.097936)\\ &+\left(\frac{5(0.4770096x+0.036763)^3-3(0.4770096x+0.036763)}{2}\right)(0.68353)\\ &+\left(\frac{35(-0.402206x-0.381068)^4-30(-0.402206x-0.381068)^2}{8}+\frac{3}{8}\right)(-0.70857)\\ &+\left(\frac{63(0.4769x-0.3459)^5-70(0.4769x-0.3459)^3}{8}+\frac{15(0.4769x-0.3459)}{8}\right)(0.63588)\\ &+\left(\frac{231(0.0521x-0.1736)^6-315(0.0521x-0.1736)^4}{16}+\frac{105(0.0521x-0.1736)^2-5}{16}\right)(-0.87063)\\ &+\left(\frac{429(-0.64453x-0.04564)^7-693(-0.64453x-0.04564)^5}{16}+\frac{315(-0.64453x-0.04564)^2-35(-0.64453x-0.04564)}{16}\right)(0.2861)\\ &+\left(\frac{6435(-0.5862x+0.3794)^8-12012(-0.5862x+0.3794)^6}{128}+\frac{6930(-0.5862x+0.3794)^4-1260(-0.5862x+0.3794)^2+35)}{128}\right)(-0.4011).\\ &+\left(\frac{12155(-0.00696x-0.0757)^9-25740(-0.00696x-0.0757)^7}{128}+\frac{18018(-0.00696x-0.0757)^5-4620(-0.00696x-0.0757)^3}{128}+\frac{315(-0.00696x-0.0757)}{128}\right)(0.4446)\\ &+\left(\frac{46189(-0.78446x-0.11764)^{10}-109395(-0.78446x-0.11764)^8}{256}+\frac{90090(-0.78446x-0.11764)^6-30030(-0.78446x-0.11764)^4}{128}+\frac{3465(-0.78446x-0.11764)^2-63}{128}\right)(0.52522)\end{aligned}$$

$$\begin{aligned}\theta_{approx}(x) &= 0.6257893 + (-0.1167977x + 0.70370075)(-0.5616733)\\ &+\left(\frac{3(0.391607x-0.976191)^2-1}{2}\right)(0.005099)\\ &+\left(\frac{5(-0.18723x-0.34599)^3-3(-0.18723x-0.34599)}{2}\right)(0.12619)\\ &+\left(\frac{35(0.5738x-0.3078)^4-30(0.5738x-0.3078)^2}{8}+\frac{3}{8}\right)(-0.41450)\\ &+\left(\frac{63(0.5707x-0.4238)^5-70(0.5707x-0.4238)^3}{8}+\frac{15(0.5707x-0.4238)}{8}\right)(-0.2190)\\ &+\left(\frac{231(-0.1313x-0.3269)^6-315(-0.1313x-0.3269)^4}{16}+\frac{105(-0.1313x-0.3269)^2-5}{16}\right)(0.45429)\\ &+\left(\frac{429(-0.36776x+0.32571)^7-693(-0.36776x+0.32571)^5}{16}+\frac{315(-0.36776x+0.32571)^2-35(-0.36776x+0.32571)}{16}\right)(-0.5598)\\ &+\left(\frac{6435(-0.00547x+0.37042)^8-12012(-0.00547x+0.37042)^6}{128}+\frac{6930(-0.00547x+0.37042)^4-1260(-0.00547x+0.37042)^2+35)}{128}\right)(0.0386).\\ &+\left(\frac{12155(-0.54871x+0.3005)^9-25740(-0.54871x+0.3005)^7}{128}+\frac{18018(-0.54871x+0.3005)^5-4620(-0.54871x+0.3005)^3}{128}+\frac{315(-0.54871x+0.3005)}{128}\right)(0.192056)\\ &+\left(\frac{46189(0.84726x+0.2779)^{10}-109395(0.84726x+0.2779)^8}{256}+\frac{90090(0.84726x+0.27794)^6-30030(0.84726x+0.2779)^4}{128}+\frac{3465(0.84726x+0.2779)^2-63}{128}\right)(0.56535)\end{aligned}$$

$$\theta_{approx}(x) = 1.04065116 + (-1.7917414x + 1.50512181)(-1.7462894)$$
$$+\left(\frac{3(0.1586005x + 1.08183793)^2 - 1}{2}\right)(0.46057357)$$
$$+\left(\frac{5(0.04384x - 0.2779)^3 - 3(0.04384x - 0.2779)}{2}\right)(0.232328)$$
$$+\left(\frac{35(-0.91334x + 0.10061)^4 - 30(-0.91334x + 0.10061)^2}{8} + \frac{3}{8}\right)(-0.24418)$$
$$+\left(\begin{array}{c}\frac{63(-0.7973x+0.20397)^5-70(-0.7973x+0.20397)^3}{8}\\ +\frac{15(-0.7973x+0.20397)}{8}\end{array}\right)(-0.88386)$$
$$+\left(\begin{array}{c}\frac{231(0.3569x-0.06613)^6-315(0.3569x-0.06613)^4}{16}\\ +\frac{105(0.3569x-0.06613)^2-5}{16}\end{array}\right)(-0.84227)$$
$$+\left(\begin{array}{c}\frac{429(1.32055x+0.11132)^7-693(1.32055x+0.11132)^5}{16}\\ +\frac{315(1.32055x+0.11132)^2-35(1.32055x+0.11132)}{16}\end{array}\right)(-1.2857)$$
$$+\left(\begin{array}{c}\frac{6435(-0.0289x+0.09457)^8-12012(-0.0289x+0.09457)^6}{128}\\ +\frac{6930(-0.0289x+0.09457)^4-1260(-0.0289x+0.09457)^2+35)}{128}\end{array}\right)(-0.15746).$$
$$+\left(\begin{array}{c}\frac{12155(-0.2899x-0.46033)^9-25740(-0.2899x-0.46033)^7}{128}\\ \frac{+18018(-0.2899x-0.46033)^5-4620(-0.2899x-0.46033)^3}{128}\\ \frac{+315(-0.2899x-0.46033)}{128}\end{array}\right)(-0.63660)$$
$$+\left(\begin{array}{c}\frac{46189(7.51E-05x-0.2764)^{10}-109395(7.51E-05x-0.2764)^8}{256}\\ \frac{+90090(7.51E-05x-0.2764)^6-30030(7.51E-05x-0.2764)^4}{128}\\ \frac{+3465(-0.2618x+0.22604)^2-63}{128}\end{array}\right)(0.39515)$$

$$\theta_{approx}(x) = 0.57174675 + (0.15215204x + 0.19122935)(0.90103211)$$
$$+\left(\frac{3(0.7133632x + 0.17390159)^2 - 1}{2}\right)(-0.5151335)$$
$$+\left(\frac{5(0.265776x + 0.299656)^3 - 3(0.265776x + 0.299656)}{2}\right)(-0.613837)$$
$$+\left(\frac{35(0.56545x + 0.642937)^4 - 30(0.56545x + 0.642937)^2}{8} + \frac{3}{8}\right)(-0.07124)$$
$$+\left(\begin{array}{c}\frac{63(0.38214x+0.28991)^5-70(0.38214x+0.28991)^3}{8}\\ +\frac{15(0.38214x+0.28991))}{8}\end{array}\right)(-0.3043)$$
$$+\left(\begin{array}{c}\frac{231(0.09838x+0.3545)^6-315(0.09838x+0.3545)^4}{16}\\ +\frac{105(0.09838x+0.3545)^2-5}{16}\end{array}\right)(-0.10316$$
$$+\left(\begin{array}{c}\frac{429(0.5656x+0.03962)^7-693(0.5656x+0.03962)^5}{16}\\ +\frac{315(0.5656x+0.03962)^2-35(0.5656x+0.03962)}{16}\end{array}\right)(0.27744)$$
$$+\left(\begin{array}{c}\frac{6435(1.81358x+0.3364)^8-12012(1.81358x+0.3364)^6}{128}\\ +\frac{6930(1.81358x+0.3364)^4-1260(1.81358x+0.3364)^2+35)}{128}\end{array}\right)(0.27103).$$
$$+\left(\begin{array}{c}\frac{12155(0.51778x+0.1045)^9-25740(0.51778x+0.1045)^7}{128}\\ \frac{+18018(0.51778x+0.1045)^5-4620(0.51778x+0.1045)^3}{128}\\ \frac{+315(0.51778x+0.1045)}{128}\end{array}\right)(-0.6385)$$
$$+\left(\begin{array}{c}\frac{46189(0.91393x+0.32061)^{10}-109395(0.91393x+0.32061)^8}{256}\\ \frac{+90090(0.91393x+0.32061)^6-30030(0.91393x+0.32061)^4}{128}\\ \frac{+3465(0.91393x+0.32061)^2-63}{128}\end{array}\right)(0.16558)$$

$$\theta_{approx}(x) = -0.37979 + (-0.239184x + 1.0147265)(0.380900)$$
$$+\left(\frac{3(-0.212776x - 0.25469)^2 - 1}{2}\right)(1.01098)$$
$$+\left(\frac{5(0.709853x - 0.2274)^3 - 3(0.709853x - 0.2274)}{2}\right)(-1.02212)$$
$$+\left(\frac{35(0.344872x - 0.34736)^4 - 30(0.344872x - 0.34736)^2}{8} + \frac{3}{8}\right)(0.53287)$$
$$+\left(\begin{array}{c}\frac{63(0.960563x-0.3200)^5-70(0.960563x-0.3200)^3}{8}\\ +\frac{15(0.960563x-0.3200))}{8}\end{array}\right)(0.783816)$$
$$+\left(\begin{array}{c}\frac{231(-0.09106x+0.18221)^6-315(-0.09106x+0.18221)^4}{16}\\ +\frac{105(-0.09106x+0.18221)^2-5}{16}\end{array}\right)(-0.75926)$$
$$+\left(\begin{array}{c}\frac{429(0.58717x-0.17318)^7-693(0.58717x-0.17318)^5}{16}\\ +\frac{315(0.58717x-0.17318)^2-35(0.58717x-0.17318)}{16}\end{array}\right)(-0.021738)$$
$$+\left(\begin{array}{c}\frac{6435(-0.00136x+0.36693)^8-12012(-0.00136x+0.36693)^6}{128}\\ +\frac{6930(-0.00136x+0.36693)^4-1260(-0.00136x+0.36693)^2+35)}{128}\end{array}\right)(0.2708).$$
$$+\left(\begin{array}{c}\frac{12155(0.01180x-0.44104)^9-25740(0.01180x-0.44104)^7}{128}\\ \frac{+18018(0.01180x-0.44104)^5-4620(0.01180x-0.44104)^3}{128}\\ \frac{+315(0.01180x-0.44104)}{128}\end{array}\right)(-0.63660)$$
$$+\left(\begin{array}{c}\frac{46189(0.00356x-0.12153)^{10}-109395(0.00356x-0.12153)^8}{256}\\ \frac{+90090(0.00356x-0.12153)^6-30030(0.00356x-0.12153)^4}{128}\\ \frac{+3465(0.00356x-0.12153)^2-63}{128}\end{array}\right)(-0.45959)$$

Approximate solution obtained by proposed algorithm for problem IV with $\lambda = 1.0, 2.0$ and 3.0 are given as

$$\theta_{approx}(x) = 0.17752421 + (0.64405052x + 1.16139197)(-0.0034589)$$
$$+\left(\frac{3(0.15493528x + 0.81978044)^2 - 1}{2}\right)(-0.151075)$$
$$+\left(\frac{5(0.003952x + 0.009672)^3 - 3(0.003952x + 0.009672)}{2}\right)(0.08889)$$
$$+\left(\frac{35(0.09809x + 0.002167)^4 - 30(0.09809x + 0.002167)^2}{8} + \frac{3}{8}\right)(0.08226)$$
$$+\left(\begin{array}{c}\frac{63(0.7103x-0.18882)^5-70(0.7103x-0.18882)^3}{8}\\ +\frac{15(0.7103x-0.18882))}{8}\end{array}\right)(0.45685)$$
$$+\left(\begin{array}{c}\frac{231(0.2266x+0.47763)^6-315(0.2266x+0.47763)^4}{16}\\ +\frac{105(0.2266x+0.47763)^2-5}{16}\end{array}\right)(-0.00279)$$
$$+\left(\begin{array}{c}\frac{429(-0.03951x+0.12464)^7-693(-0.03951x+0.12464)^5}{16}\\ +\frac{315(-0.03951x+0.12464)^2-35(-0.03951x+0.12464)}{16}\end{array}\right)(0.93020)$$
$$+\left(\begin{array}{c}\frac{6435(0.0223x+0.77849)^8-12012(0.0223x+0.77849)^6}{128}\\ +\frac{6930(0.0223x+0.77849)^4-1260(0.0223x+0.77849)^2+35)}{128}\end{array}\right)(0.00359).$$
$$+\left(\begin{array}{c}\frac{12155(0.00051x+0.97125)^9-25740(0.00051x+0.97125)^7}{128}\\ \frac{+18018(0.00051x+0.97125)^5-4620(0.00051x+0.97125)^3}{128}\\ \frac{+315(0.00051x+0.97125)}{128}\end{array}\right)(-0.01223)$$
$$+\left(\begin{array}{c}\frac{46189(-3.06E-06x+0.44788)^{10}-109395(-3.06E-06x+0.44788)^8}{256}\\ \frac{+90090(-3.06E-06x+0.44788)^6-30030(-3.06E-06x+0.44788)^4}{128}\\ \frac{+3465(-3.06E-06x+0.44788)^2-63}{128}\end{array}\right)(0.0026)$$

$$\theta_{approx}(x) = 0.13882379 + (-0.7640621x - 0.0236816)(-0.00388855)$$
$$+\left(\frac{3(-0.7633091x - 0.1350345)^2 - 1}{2}\right)(-0.88167506)$$
$$+\left(\frac{5(-0.8665x + 0.126274)^3 - 3(-0.8665x + 0.126274)}{2}\right)(0.19184)$$
$$+\left(\frac{35(0.098156x - 0.01684)^4 - 30(0.098156x - 0.01684)^2}{8} + \frac{3}{8}\right)(-0.00882)$$
$$+\left(\begin{array}{c}\frac{63(0.2841x+0.14442)^5-70(0.2841x+0.14442)^3}{8}\\ +\frac{15(0.2841x+0.14442))}{8}\end{array}\right)(-0.02870)$$
$$+\left(\begin{array}{c}\frac{231(0.2838x-0.2359)^6-315(0.2838x-0.2359)^4}{16}\\ +\frac{105(0.2838x-0.2359)^2-5}{16}\end{array}\right)(-0.29817)$$
$$+\left(\begin{array}{c}\frac{429(0.1373x-0.75418)^7-693(0.1373x-0.75418)^5}{16}\\ +\frac{315(0.1373x-0.75418)^2-35(0.1373x-0.75418)}{16}\end{array}\right)(-0.4103)$$
$$+\left(\begin{array}{c}\frac{6435(9.40E-05x-0.1211)^8-12012(9.40E-05x-0.1211)^6}{128}\\ +\frac{6930(9.40E-05x-0.1211)^4-1260(9.40E-05x-0.1211)^2+35)}{128}\end{array}\right)(-0.7390).$$
$$+\left(\begin{array}{c}\frac{12155(0.0352x-0.45569)^9-25740(0.0352x-0.45569)^7}{128}\\ +\frac{18018(0.0352x-0.45569)^5-4620(0.0352x-0.45569)^3}{128}\\ +\frac{315(0.0352x-0.45569)}{128}\end{array}\right)(-0.07844)$$
$$+\left(\begin{array}{c}\frac{46189(0.00123x+0.02433)^{10}-109395(0.00123x+0.02433)^8}{256}\\ +\frac{90090(0.00123x+0.02433)^6-30030(0.00123x+0.02433)^4}{128}\\ +\frac{3465(0.00123x+0.02433)^2-63}{128}\end{array}\right)(-0.98536)$$

REFERENCES

[1] AD Kraus, A Aziz, and J Welty. Heat transfer considerations. Extended Surface Heat Transfer, John Wiley & Sons, New York, 2002.

[2] DW Mueller Jr and Hosni I Abu-Mulaweh. Prediction of the temperature in a fin cooled by natural convection and radiation. Applied Thermal Engineering, 26(14-15):1662–1668, 2006.

[3] AS Dogonchi et al. Heat transfer by natural convection of fe3o4-water nanofluid in an annulus between a wavy circular cylinder and a rhombus. International Journal of Heat and Mass Transfer, 130:320–332, 2019.

[4] M Ijaz Khan, Sumaira Qayyum, S Kadry, WA Khan, and SZ Abbas. Irreversibility analysis and heat transport in squeezing nanoliquid flow of non-newtonian (second-grade) fluid between infinite plates with activation energy. Arabian Journal for Science and Engineering, 45(6):4939–4947, 2020.

[5] MK Nayak, AK Abdul Hakeem, B Ganga, M Ijaz Khan, Muhammad Waqas, and Oluwole Daniel Makinde. Entropy optimized mhd 3d nanomaterial of non-newtonian fluid: a combined approach to good absorber of solar energy and intensification of heat transport. Computer methods and programs in biomedicine, 186:105131, 2020.

[6] MI Khan and F Alzahrani. Transportation of heat through cattaneo-christov heat flux model in non-newtonian fluid subject to internal resistance of particles. Applied Mathematics and Mechanics, 41(8):1157–1166, 2020.

[7] M Ijaz Khan and Faris Alzahrani. Cattaneo-christov double diffusion (ccdd) and magnetized stagnation point flow of non-newtonian fluid with internal resistance of particles. Physica Scripta, 95(12):125002, 2020.

[8] M Ijaz Khan. Transportation of hybrid nanoparticles in forced convective darcy-forchheimer flow by a rotating disk. International Communications in Heat and Mass Transfer, 122:105177, 2021.

[9] Ahmad Zeeshan, Nasir Shehzad, Rahmat Ellahi, and Sultan Z Alamri. Convective poiseuille flow of al 2 o 3-eg nanofluid in a porous wavy channel with thermal radiation. Neural Computing and Applications, 30(11):3371–3382, 2018.

[10] NZAERVK Shehzad, A Zeeshan, R Ellahi, and K Vafai. Convective heat transfer of nanofluid in a wavy channel: Buongiorno's mathematical model. Journal of Molecular Liquids, 222:446–455, 2016.

[11] Ching-Huang Chiu et al. A decomposition method for solving the convective longitudinal fins with variable thermal conductivity. International Journal of Heat and Mass Transfer, 45(10):2067–2075, 2002.

[12] Cihat Arslanturk. A decomposition method for fin efficiency of convective straight fins with temperature-dependent thermal conductivity. International Communications in Heat and Mass Transfer, 32(6):831–841, 2005.

[13] A Rajabi, DD Ganji, and H Taherian. Application of homotopy perturbation method in nonlinear heat conduction and convection equations. Physics Letters A, 360(4-5):570–573, 2007.

[14] DD Ganji, M Rahimi, and M Rahgoshay. Determining the fin efficiency of convective straight fins with temperature dependent thermal conductivity by using homotopy perturbation method. International Journal of Numerical Methods for Heat & Fluid Flow, 2012.

[15] F Khani and Abdul Aziz. Thermal analysis of a longitudinal trapezoidal fin with temperature-dependent thermal conductivity and heat transfer coefficient. Communications in Nonlinear Science and Numerical Simulation, 15(3):590–601, 2010.

[16] DD Ganji, GA Afrouzi, and RA Talarposhti. Application of variational iteration method and homotopy–perturbation method for nonlinear heat diffusion and heat transfer equations. Physics Letters A, 368(6):450–457, 2007.

[17] Safa Bozkurt Coşkun and Mehmet Tarık Atay. Fin efficiency analysis of convective straight fins with temperature dependent thermal conductivity using variational iteration method. Applied Thermal Engineering, 28(17-18):2345–2352, 2008.

[18] AA Joneidi, DD Ganji, and M Babaelahi. Differential transformation method to determine fin efficiency of convective straight fins with temperature dependent thermal conductivity. International Communications in Heat and Mass Transfer, 36(7):757–762, 2009.

[19] MG Sobamowo. Thermal analysis of longitudinal fin with temperature-dependent properties and internal heat generation using galerkin's method of weighted residual. Applied Thermal Engineering, 99:1316–1330, 2016.

[20] Sin Kim and Cheng-Hung Huang. A series solution of the non-linear fin problem with temperature-dependent thermal conductivity and heat transfer coefficient. Journal of Physics D: Applied Physics, 40(9):2979, 2007.

[21] RJ Moitsheki, T Hayat, and MY Malik. Some exact solutions of the fin problem with a power law temperature-dependent thermal conductivity. Nonlinear Analysis: Real World Applications, 11(5):3287–3294, 2010.

[22] Saeid Abbasbandy and Elyas Shivanian. Exact closed form solutions to nonlinear model of heat transfer in a straight fin. International Journal of Thermal Sciences, 116:45–51, 2017.

[23] Sheng-Wei Sun and Xian-Fang Li. Exact solution of a nonlinear fin problem of temperature-dependent thermal conductivity and heat transfer coefficient. Canadian Journal of Physics, 98(7):700–712, 2020.

[24] M Ijaz Khan, Mubbashar Nazeer, Nasir Shehzad, Adila Saleem, and Fayyaz Ahmad. Scrutiny of entropy optimized tangent hyperbolic fluid (non-newtonian) through perturbation and numerical methods between heated plates. Advances in Mechanical Engineering, 12(12):1687814020970772, 2020.

[25] Ahmad Zeeshan Kohilavani Naganthran, Md Faisal Md Basir, Nasir Shehzad, Roslinda Nazar, Rakesh Choudhary, and Sankarasubramanian Balaji. Concentration flux dependent on radiative mhd casson flow with arrhenius activation energy: Homotopy analysis method (ham) with an evolutionary algorithm. Journal homepage: http://iieta. org/journals/ijht, 38(4):785–793, 2020.

[26] M Ijaz Khan and Faris Alzahrani. Binary chemical reaction with activation energy in dissipative flow of non-newtonian nanomaterial. Journal of Theoretical and Computational Chemistry, 19(03):2040006, 2020.

[27] Muhammad Ibrahim and M Ijaz Khan. Mathematical modeling and analysis of swcnt-water and mwcnt-water flow over a stretchable sheet. Computer methods and programs in biomedicine, 187:105222, 2020.

[28] M Ijaz Khan and Faris Alzahrani. Activation energy and binary chemical reaction effect in nonlinear thermal radiative stagnation point flow of walter-b nanofluid: Numerical computations. International Journal of Modern Physics B, 34(13):2050132, 2020.

[29] M Ijaz Khan and Faris Alzahrani. Free convection and radiation effects in nanofluid (silicon dioxide and molybdenum disulfide) with second order velocity slip, entropy generation, darcy-forchheimer porous medium. International Journal of Hydrogen Energy, 46(1):1362–1369, 2021.

[30] M Ijaz Khan and Faris Alzahrani. Entropy optimized magnetohydrodynamics darcy–forchheimer second order velocity slip flow of nanomaterials between two stretchable disks. Proceedings of the Institution of Mechanical Engineers, Part C: Journal of Mechanical Engineering Science, 234(21):4190–4199, 2020.

[31] Mohsen Torabi, Hessameddin Yaghoobi, and A Aziz. Analytical solution for convective–radiative continuously moving fin with temperature-dependent thermal conductivity. International Journal of Thermophysics, 33(5):924–941, 2012.

[32] Sobhan Mosayebidorcheh and Taha Mosayebidorcheh. Series solution of convective radiative conduction equation of the nonlinear fin with temperature dependent thermal conductivity. International Journal of Heat and Mass Transfer, 55(23-24):6589–6594, 2012.

[33] A Aziz, Mohsen Torabi, and Kaili Zhang. Convective–radiative radial fins with convective base heating and convective–radiative tip cooling: homogeneous and functionally graded materials. Energy Conversion and Management, 74:366–376, 2013.

[34] Mo Miansari, DD Ganji, and Me Miansari. Application of he's variational iteration method to nonlinear heat transfer equations. Physics Letters A, 372(6):779–785, 2008.

[35] Jing Ma, Yasong Sun, and Benwen Li. Simulation of combined conductive, convective and radiative heat transfer in moving irregular porous fins by spectral element method. International Journal of Thermal Sciences, 118:475–487, 2017.

[36] SA Atouei, Kh Hosseinzadeh, M Hatami, Seiyed E Ghasemi, SAR Sahebi, and DD Ganji. Heat transfer study on convective–radiative semi-spherical fins with temperature-dependent properties and heat generation using efficient computational methods. Applied Thermal Engineering, 89:299–305, 2015.

[37] AR Shateri and B Salahshour. Comprehensive thermal performance of convection–radiation longitudinal porous fins with various profiles and multiple nonlinearities. International Journal of Mechanical Sciences, 136:252–263, 2018.

[38] MN Bouaziz and Abdul Aziz. Simple and accurate solution for convective–radiative fin with temperature dependent thermal conductivity using double optimal linearization. Energy Conversion and Management, 51(12):2776–2782, 2010.

[39] Yong Huang and Xian-Fang Li. Exact and approximate solutions of convective-radiative fins with temperature-dependent thermal conductivity using integral equation method. International Journal of Heat and Mass Transfer, 150:119303, 2020.

[40] Mohsen Torabi and A Aziz. Thermal performance and efficiency of convective–radiative t-shaped fins with temperature dependent thermal conductivity, heat transfer coefficient and surface emissivity. International Communications in Heat and Mass Transfer, 39(8):1018–1029, 2012.

[41] Ranjan Das and Balaram Kundu. Forward and inverse nonlinear heat transfer analysis for optimization of a constructal t-shape fin under dry and wet conditions. International Journal of Heat and Mass Transfer, 137:461–475, 2019.

[42] Raj Bahadur and Avram Bar-Cohen. Orthotropic thermal conductivity effect on cylindrical pin fin heat transfer. In International Electronic Packaging Technical Conference and Exhibition, volume 42002, pages 245–252, 2005.

[43] Abdul Aziz and OD Makinde. Heat transfer and entropy generation in a two-dimensional orthotropic convection pin fin. International Journal of Exergy, 7(5):579–592, 2010.

[44] Kuljeet Singh, Ranjan Das, and Balaram Kundu. Approximate analytical method for porous stepped fins with temperature-dependent heat transfer parameters. Journal of Thermophysics and Heat Transfer, 30(3):661–672, 2016.

[45] Rohit K Singla and Ranjan Das. A differential evolution algorithm for maximizing heat dissipation in stepped fins. Neural Computing and Applications, 30(10):3081–3093, 2018.

[46] T Hayat, M Ijaz Khan, M Farooq, A Alsaedi, M Waqas, and Tabassam Yasmeen. Impact of cattaneo–christov heat flux model in flow of variable thermal conductivity fluid over a variable thicked surface. International Journal of Heat and Mass Transfer, 99:702–710, 2016.

[47] MD Mhlongo, RJ Moitsheki, and OD Makinde. Transient response of longitudinal rectangular fins to step change in base temperature and in base heat flow conditions. International Journal of Heat and Mass Transfer, 57(1):117–125, 2013.

[48] Balaram Kundu, Ranjan Das, Pramod A Wankhade, and Kwan-Soo Lee. Heat transfer improvement of a wet fin under transient response with a unique design arrangement aspect. International Journal of Heat and Mass Transfer, 127:1239–1251, 2018.

[49] Pramod A Wankhade, Balaram Kundu, and Ranjan Das. Establishment of non-fourier heat conduction model for an accurate transient thermal response in wet fins. International Journal of Heat and Mass Transfer, 126:911–923, 2018.

[50] Muhammad Ijaz Khan, Muhammad Waqas, Tasawar Hayat, and Ahmed Alsaedi. A comparative study of casson fluid with homogeneous-heterogeneous reactions. Journal of colloid and interface science, 498:85–90, 2017.

[51] M Ijaz Khan and Faris Alzahrani. Entropy-optimized dissipative flow of carreau–yasuda fluid with radiative heat flux and chemical reaction. The European Physical Journal Plus, 135(6):1–16, 2020.

[52] M Ijaz Khan and Faris Alzahrani. Nonlinear dissipative slip flow of jeffrey nanomaterial towards a curved surface with entropy generation and activation energy. Mathematics and Computers in Simulation, 185:47–61, 2021.

[53] M Ijaz Khan and Faris Alzahrani. Dynamics of activation energy and nonlinear mixed convection in darcy-forchheimer radiated flow of carreau nanofluid near stagnation point region. Journal of Thermal Science and Engineering Applications, 13(5):051009, 2021.

[54] Muhammad Ijaz Khan and Faris Alzahrani. Numerical simulation for the mixed convective flow of non-newtonian fluid with activation energy and entropy generation. Mathematical Methods in the Applied Sciences, 44(9):7766–7777, 2021.

[55] Wen Huang, Tianhua Jiang, Xiucheng Zhang, Naveed Ahmad Khan, and Muhammad Sulaiman. Analysis of beam-column designs by varying axial load with internal forces and bending rigidity using a new soft computing technique. Complexity, 2021, 2021.

[56] Waseem Waseem, Muhammad Sulaiman, Poom Kumam, Muhammad Shoaib, Muhammad Asif Zahoor Raja, and Saeed Islam. Investigation of singular ordinary differential equations by a neuroevolutionary approach. Plos one, 15(7):e0235829, 2020.

[57] Naveed Ahmad Khan, Muhammad Sulaiman, Poom Kumam, and Abdulah Jeza Aljohani. A new soft computing approach for studying the wire coating dynamics with oldroyd 8-constant fluid. Physics of Fluids, 33(3):036117, 2021.

[58] Ashfaq Ahmad, Muhammad Sulaiman, Ahmad Alhindi, and Abdulah Jeza Aljohani. Analysis of temperature profiles in longitudinal fin designs by a novel neuroevolutionary approach. IEEE Access, 8:113285–113308, 2020.

[59] Waseem Waseem, Muhammad Sulaiman, Saeed Islam, Poom Kumam, Rashid Nawaz, Muhammad Asif Zahoor Raja, Muhammad Farooq, and Muhammad Shoaib. A study of changes in temperature profile of porous fin model using cuckoo search algorithm. Alexandria Engineering Journal, 59(1):11–24, 2020.

[60] W Waseem, Muhammad Sulaiman, Ahmad Alhindi, and Hosam Alhakami. A soft computing approach based on fractional order dpso algorithm designed to solve the corneal model for eye surgery. IEEE Access, 8:61576–61592, 2020.

[61] Zhang Yin, Jianqiang Lin, Zhenhuan Hu, Naveed Ahmad Khan, and Muhammad Sulaiman. Analysis of third-order nonlinear multi-singular emden–fowler equation by using the lenn-woa-nm algorithm. IEEE Access, 2021.

[62] Amjad Ali, Muhammad Hamraz, Poom Kumam, Dost Muhammad Khan, Umair Khalil, Muhammad Sulaiman, and Zardad Khan. A k-nearest neighbours based ensemble via optimal model selection for regression. IEEE Access, 8:132095–132105, 2020.

[63] Muhammad Sulaiman, Masihullah MASİHULLAH, Zubair Hussain, Sohail Ahmad, Wali Khan Mashwani, Muhammad Asif Jan, and Rashida Adeeb Khanum. Implementation of improved grasshopper optimization algorithm to solve economic load dispatch problems. Hacettepe Journal of Mathematics and Statistics, 48(5):1570–1589, 2019.

[64] Ayaz Hussain Bukhari, Muhammad Asif Zahoor Raja, Muhammad Sulaiman, Saeed Islam, Muhammad Shoaib, and Poom Kumam. Fractional neuro-sequential arfima-lstm for financial market forecasting. IEEE Access, 8:71326–71338, 2020.

[65] Muhammad Sulaiman, Ashfaq Ahmad, Asfandyar Khan, and Shakoor Muhammad. Hybridized symbiotic organism search algorithm for the optimal operation of directional overcurrent relays. Complexity, 2018, 2018.

[66] Muhammad Sulaiman, Ismat Samiullah, Ab Hamdi, and Zubair Hussain. An improved whale optimization algorithm for solving multi-objective design optimization problem of pfhe. Journal of Intelligent & Fuzzy Systems, 37(3):3815–3828, 2019.

[67] Ayaz Hussain Bukhari, Muhammad Sulaiman, Saeed Islam, Muhammad Shoaib, Poom Kumam, and Muhammad Asif Zahoor Raja. Neuro-fuzzy modeling and prediction of summer precipitation with application to different meteorological stations. Alexandria Engineering Journal, 59(1):101–116, 2020.

[68] Hassan Javed, Muhammad Asif Jan, Nasser Tairan, Wali Khan Mashwani, Rashida Adeeb Khanum, Muhammad Sulaiman, Hidayat Ullah Khan, and Habib Shah. On the efficacy of ensemble of constraint handling techniques in self-adaptive differential evolution. Mathematics, 7(7):635, 2019.

[69] Naveed Ahmad Khan, Muhammad Sulaiman, Abdulah Jeza Aljohani, Poom Kumam, and Hussam Alrabaiah. Analysis of multi-phase flow

through porous media for imbibition phenomena by using the lenn-woa-nm algorithm. IEEE Access, 8:196425–196458, 2020.

[70] A Muzzio. Approximate solution for convective fins with variable thermal conductivity. ASME Transactions Journal of Heat Transfer, 98:680–682, 1976.

[71] Cai-Ning Zhang and Xian-Fang Li. Temperature distribution of conductive-convective-radiative fins with temperature-dependent thermal conductivity. International Communications in Heat and Mass Transfer, 117:104799, 2020.

[72] Eric W Weisstein. Legendre polynomial. Mathematical Methods, page 43, 2015.

[73] Seyedali Mirjalili and Andrew Lewis. The whale optimization algorithm. Advances in engineering software, 95:51–67, 2016.

[74] Saša Singer and John Nelder. Nelder-mead algorithm. Scholarpedia, 4(7):2928, 2009.

[75] Raka Jovanovic, Sabre Kais, and Fahhad H Alharbi. Cuckoo search inspired hybridization of the nelder-mead simplex algorithm applied to optimization of photovoltaic cells. arXiv preprint arXiv:1411.0217, 2014.

[76] Ranjan Das. A simplex search method for a conductive–convective fin with variable conductivity. International Journal of Heat and Mass Transfer, 54(23-24):5001–5009, 2011.